Sudan University of Science and Technology
College of graduate Studies
College of Petroleum Engineering and Technology
Petroleum Engineering Department

Integrated Formation Evaluation of South Annajma Field, Muglad Basin,Sudan

تقييم التكوينات المتكاملة المنتجة بحقل النجمة جنوب-حوض المجلد-السودان

A Thesis submitted as a Partial fulfillment to the Admission of the Degree of Master in Petroleum Engineering reservoir

By:
Zeinab Faisal Abdalrazig

Supervisor:
D.Ali Sayed Mohammed

June, 2016

الإستهلال

قال تعالى :

(يرفع الله الذين آمنو منكم والذين أوتو العلم درجات والله بما تعملون خبير) .

صدق الله العظيم

سورة المجادلة

الإهداء

إلى كل من أضاء بعلمه عقل غيره

أو هدى بالجواب الصحيح حيرة سائليه

فأظهر بسماحته تواضع العلماء

وبرحابته سماحه العارفين

إلى النور الذي ينير لي درب النجاح

أبي

إلى من علمتني الصمود مهما تبدلت الظروف

أمي

إلى أساتذتي وكل من علمني حرفا

أهدي هذا العمل المتواضع راجيا المولى عز وجل

أن يجد القبول والنجاح

شكر وعرفان

ربي أوزعني ان أشكر نعمتك التي أنعمت علي وعلى والدي وأن أعمل صالحا ترضاه وأدخلني برحمتك في عبادك الصالحين .

الشكر الجزيل لكل من ساهم معي في إنجاز هذه الدراسه واخص بخالص الشكر والتقدير :

د / علي السيد

م/ مصطفي حمد عيسي

م/ محمد ميرغني محمد علي

CONTENT

Chapter 1: Introduction

1.1. Formation evaluation ……..... 1

1.2. Coring ……..... 2

1.2.1 Routine or Conventional Core Analysis Test …….. 2

1.2.2 Special Core Analysis Test (SCAL) ……... 2

1.3. Well logging
…… 3

1.4. General Objectives of the Study ……. 4

1.5 Special objectives ……..... 4

1.6. Introduction to case study.....……..... 5

Chapter two: Literature Review and Theoretical Background

2.1. Literature Review …….. 6

2.2. Geological Development of NE Africa & Tectonic and StructuralFramework……...10

2.3. Rifting in Sudan……...……..11

2.3.1. Pre-rifting Phase…….12

2.3.2. Rifting Phases…….12

2.3.3. The Sag Phase……..……..14

2.4. The effect of the rifting phases in Melut basin……..15

2.5. Stratigraphy of Melut Basin……...16

2.5.1. Lower Cretaceous…….17

2.5.2. Upper Cretaceous…….17

2.5.3. Paleogene……17

2.5.4. Neogene Quaternary……..……..18

Chapter 3: Reservoir characterization from wireline logging & core analysis

3.1. Introduction…….19

3.2. Porosity……...21

3.2.1. Porosity from wireline logging ……..…22

3.2.1.1. Density Log…….22

3.2.1.2. Neutron Log……23

3.2.1.3. Acoustic Log ……..25

3.2.2. Porosity form core analysis……..27

3.2.2.1 Experiment 1: Effective porosity determination by helium porosimeter method:…….27

3.2.2.2. Experiment 2: Porosity determination by liquid saturating method: ……....28 3.3.
Resistivity……..30

3.3.1. Resistivity from wireline logging……..32

3.3.1.1. Conventional Resistivity Logging……..….32

3.3.2. Resistivity From core analysis

3.3.2.1. Experiment: Resistivity measurements of fluid- saturated rocks……34

3.4. Permeability……...36

3.4.1. Determination of permeable zones using wireline logging ……36

3.4.1.1. Gamma Ray……..36

3.4.1.2. Caliper Logs……...39

3.4.1.3. Spontaneous potential log(SP)…….41

3.4.2. Measurement of Permeability using core analysis……...45

3.4.2.1. Experiment: Absolute permeability measurement of water……...……45

3.4.3. Relative permeability from core analysis……..46

3.4.3.1. Steady State Method…….47

3.4.3.2. Unsteady State Method…….47

Chapter 4: Interpretation & calculation

4.1. Introduction…….49

4.2. Wireline logging manual interpretation…….49

4.2.1. Lithology identification……...49

4.2.2. Porosity calculation from porosity logs …….51

4.2.3. Calculation the saturation from resistivity logs……...56

4.2.4. Shale volume from gamma ray log ……...64

4.3. Wireline logging interpretation using interactive petrophysics software……68

4.4. Core analysis data……..78

Chapter 5 :Result and Discussion

5.1. Original Oil In Place (OOIP)……...……..82

5.1.1. Parameter Used In Calculation of (OOIP)……83

5.1.2. Calculation Of Original Oil In Place (OOIP)……...84

Conclusion……..86

Recommendations……...87

References……………………………………………………………...88
Appendix……………..……………………………………………..89

ABSTRACT

In petroleum engineering and, formation Evaluation is used to determine the ability of borehole to produce petroleum. Essentially, it is the process of 'recognizing a commercial well when you drill one.

The most common petrophysical exercises used in evaluating reservoirs and assessing reserves are log analysis, core measurements. In this research the special core analysis (SCAL) and well logging data was used to evaluate Bentiu Formation from Muglad Basin in Sudan which is shelly sand reservoirs.

A prelude of this research was containing introduction ,and then the well logging data (from three wells (south Annajma 3, south Annajma 7, south Annajma 17) used to calculate the petrophysical properties by using Interactive Petrophysics "IP" and then compared with relative permeability and capillary pressure analysis from core samples data.

The calculated petrophysical properties include porosity, Volume of shale, and water saturation, and core analysis data include porosity, water saturation, residual oil saturation ,water permeability at residual oil saturation, oil permeability at initial water saturation and transition zone height . Capillary pressure analyses confirm that the production from these formations will be two phase (Oil + Water) from the beginning of the production.

CHAPTER 1

INTRODUCTION

What is Formation Evaluation?

Formation Evaluation (FE) is the process of interpreting a combination of measurements taken inside a wellbore to detect and quantify oil and gas reserves in the rock adjacent to the well. FE data can be gathered with wireline logging instruments or logging-while-drilling tools.

- Study of the physical properties of rocks and the fluids contained within them.
- Data are organized and interpreted by depth and represented on a graph called a log (a record of information about the formations through which a well has been drilled).

The search or economic accumulations of oil and gas starts with the recognition of likely geological provinces, progresses to seismic surveying, and the drilling of one or more wild-cat wells. If one is lucky, these wells may encounter oil, and if that is the case, measurements made down the hole with wireline tools are used to assess whether sufficient oil is present, and whether it can be produced. Clearly, the evaluation of sub-surface formations requires the combined efforts of geologists, petrophysicists, drilling engineers and even geophysicists

1.1 Formation Evaluation

In petroleum exploration and development, formation evaluation is used to determine the ability of a borehole to produce petroleum .Essentially; it is the process of "recognizing a commercial well when you drill one.

The formation evaluation process should answer two questions:

- What are the lower limits for porosity, permeability, and upper limits for water saturation that permit profitable production from a particular formation or pay zone?
- Do any of the formations in the well under consideration exceed these lower limits?

Sources of Formation Evaluation Data:

- Analaogy
- Mud Logging

- Coring
- Open hole Logging
- Well Testing
- Production History

1.2 Coring

A core is a sample of a rock from the well section, generally obtained by drilling into the formation with a hollow section drill pipe and drill bit.

Core operation: there are two core methods are practiced: conventional and wireline coring

Conventional coring Which refers to core taken without regard to precise orientation , encompasses arrange of coring device and core barrels .the main Advantages of conventional coring is that the entire drill string be Pulled to retrieve the core ; however , the corresponding is that larg Cores , 3to5 in diameter and 30to90 long , may be recovered .

Wireline coring: Two wireline tools are currently used: sidewall core gun, and the Rotary sidewall coring tool. Sidewall coring is necessary when it is desirable to obtain core sample From a particular zone already drilled, especially in soft rock zones Where hole conditions are not conductive to open hole drill stem testing The second tool is the rotary sidewall coring tool .this tool uses a motorized bit to drill into the borehole wall to retrieve its sample It can cut 30 core sample per trip. Core size is 15/16 in diameter and 2 in long. This device works better than the sidewall core gun in consolidate formations.

Core preservation: the objective of core preservation is to retain the wettability condition of a recovered core sample, and to prevent change in petrophysical character.

Core analysis: There are basically two main categories of core analysis tests that are performed on core samples regarding physical properties of Reservoir rocks are:

1.2.1 Routine or Conventional Core Analysis Test:

Its primary concerned with establishing the variation of porosity and Permeability as a function of position and depth in a well.

The core is usually slabbed, cut lengthwise to make the structure visible. Provides information on lithology, residual fluid saturation, ambient porosity, ambient gas permeability and grain density.

1.2.2 Special Core Analysis Test (SCAL):

What is special core analysis? to some special core analysis is include any analysis other than routine core analysis , i.e. measurements other than porosity ,permeability and grain density .according to the definition the following would fall within special core analysis : rock and pore volume compressibility , electrical properties , displacement tests including water/oil and gas/oil relative permeability , capillary pressure , trapped gas saturation , the effect of net confining pressure on rock properties and tests of water compatibility .

To others special core analysis refers to those analyses which are dependent on fluid saturation and/or wettability, and in particular to capillary pressure and relative permeability.

While either of these definitions are acceptable, the second more restricted definition is used in this research, i.e. we will deal primary with relative permeability and capillary pressure. Many of the concepts presented in, however, and particularly those relating to characterization of reservoir rocks, can be applied to other measurements as well.

1.3 Well logging:

Logging, electro logging or well logging means continuous recording of a physical parameter of the formation with depth.

Logs are made by Moving a tool string at a certain logging speed, and recording data at certain intervals called sampling rate. – The “log” is the recording of each of these data samples at a recorded depth.

The primary objectives of the wire line logging are

- The identification of reservoir
- The estimation of hydrocarbon in place.
- The estimation of recoverable hydrocarbon.

Well logs are results of several geophysical measurements recorded in a well bore. They consist of key information about formation drilled i.e.

1. To identify the productive zones of hydrocarbon.
2. To define the petrophysical parameters like porosity, permeability, hydrocarbon, saturation and lithology of zones.
3. To determine depth, thickness, formation temperature and pressure of a reservoir.
4. To distinguish between oil, gas and water zones in a reservoir.
5. To measure hydrocarbon mobility.

Standard Logging:

- Formation Gamma Ray
- Neutron Porosity
- Density (Porosity)
- Caliper (hole size)
- Pad Resistivity (good resolution)
- Resistivity (good depth investigation)
- Spontaneous Potential Mud Resistivity

1.4 General Objectives of the Study:

The overall objective of the study is to review existing dataset and to perform integrated formation evaluation for the potential zones expected in Bentiu Formations for the two wells at South Annajma Field

1.5 Special objectives:

1. Confirm the initial water saturation and residual oil saturation values from relative permeability curve
2. Determine the wettability and water saturation log equation using capillary pressure curve results.
3. Determine reservoir properties (Shale content of the objective sections, porosity, permeability, and water saturation) from well logging data analysis.

1.6 Introduction to case study:

The South Annajma field is located in block 17 in the south west of Sudan; Seismic data acquired and number of wells has been drilled on the field, which lead to the discovery and lately to commercial production of the field.

The data will include: drilling reports, well logs, mud log, cuttings analysis, Core analysis reports, testing.

CHAPTER 2

LITERATURE REVIEW AND THEORETICAL BACKGROUND

2.1 Literature Review:

The capabilities and number of new formation evaluation tools and interpretation methods that have become available since the early 1990s are impressive. These advancements speak to the focused effort the petroleum industry has made to become more efficient by judiciously applying the latest technological developments to increase hydrocarbon recovery and to lower finding and producing costs in a safe and environmentally appropriate manner. In 1971, Jordan, J.R., defined the formation evaluation as "the determination of the economic worth of a natural resource occurring in the subsurface", and indicated that the in-place value of petroleum reservoir is defined by its primary properties: its areal extent and thickness, its pore size distribution, its fluid distribution, and the composition of hydrocarbon fluids. In 1979, Pelissier-Combescure, J., Pollock, D., Wittmann, M., discussed the application of Repeat Formation Tester application in determination of reservoir pressure, fluid density, fluid contacts, differential depletion, reservoir inter-communication and effective permeability's of invaded and uninvaded zones. They also illustrated the phenomenon of supercharging "the effect of filtrate invasion" with field examples. The data generated from special-core-analysis (SCAL) tests have a significant impact on the

development of reservoir engineering models. The main goal of coring is to retrieve core samples from a well to get the maximum amount of information about the reservoir. Core samples collected provide important petrophysical, petrographic, paleontological, sedimentological, and digenetic information. In 2006, S. Siddiqui, T.M. Okasha, J.J. Funk, and A.M. Al-Harbi, describes some of the criteria and tests required for the selection of representative samples for use in SCAL tests. The proposed technique ensures that high-quality core plugs are chosen to represent appropriate flow compartments or fancies within the reservoir.

In 2011, H.Mosab , A.M. Ahmad describes the formation evaluation using conventional and special core analysis and the results determine the residual oil saturation and initial water saturation accurately.

In 2013, A.Abdallah, H.A. Hamid and W.M. Jaber describe formation evaluation using special core analysis and repeat formation test they determine the true value of the residual oil saturation and water saturation also the interpretation of relative permeability curve and capillary pressure curve and determine the optimum perforation zone.

My study will use the same strategy to interpretation of capillary pressure and relative permeability curves but the addition will be using the interactive petrophysics software to compare the results and insure them also to determine the shale content, porosity, water saturation and net reservoir pay.

2.2 Overview of some important concepts:

The material of which a petroleum reservoir rock may be composed can range from very loose and unconsolidated sand to a very hard and dense sandstone, limestone, or dolomite. The grains may be bonded together with a number of materials, the most common of which are Silica, calcite, or clay. Knowledge of the physical properties of the rock and the existing interaction between the hydrocarbon system and the formation is essential in understanding and evaluating the performance of a given reservoir.

2.3 Porosity

The porosity of a rock is a measure of the storage capacity (pore volume) that is capable of holding fluids. Quantitatively, the porosity is the ratio of the pore volume to the total volume

(bulk volume). This important rock property is determined mathematically by the following generalized relationship:

$$\varphi = \frac{pore\ volume}{bulk\ volume} \quad \text{…….. (2.1)}$$

Where φ=porosity

As the sediments were deposited and the rocks were being formed during past geological times, some void spaces that developed became isolated from the other void spaces by excessive cementation. Thus, many of the void spaces are interconnected while some of the pore spaces are completely isolated. This leads to two distinct types of porosity, namely:

• Absolute porosity

• Effective porosity

2.3.1 Absolute porosity:

The absolute porosity is defined as the ratio of the total pore space in the rock to that of the bulk volume. A rock may have considerable absolute porosity and yet have no conductivity to fluid for lack of pore interconnection. The absolute porosity is generally expressed mathematically by the following relationships:

$$\Phi a = \frac{\text{total pore volume}}{\text{bulk volume}} \quad \text{……. (2.2)}$$

Where φa-= absolute porosity.

2.3.2 Effective porosity:

The effective porosity is the percentage of interconnected pore space with respect to the bulk volume, or

$$\varphi = \frac{\text{interconnected pore volume}}{\text{bulk volume}} \text{ …… (2.3)}$$

Where φ=effective porosity.

The effective porosity is the value that is used in all reservoir engineering calculations because it represents the interconnected pore space that contains the recoverable hydrocarbon fluids. Porosity may be classified according to the mode of origin as originally induced. The original porosity is that developed in the deposition of the material, while induced porosity is that developed by some geological process sub- sequent to deposition of the rock. The intergranular porosity of sandstones and the intercrystalline and oolitic porosity of some limestones typify original porosity. Induced porosity is typified by fracture development as found in shales and limestones and by the slugs or solution cavities commonly found in limestones. Rocks having original porosity are more uniform in their characteristics than those rocks in which a large part of the porosity is included. For direct quantitative measurement of porosity, reliance must be placed on formation samples obtained by coring. Since effective porosity is the porosity value of interest to the petroleum engineer, particular attention should be paid to the methods used to determine porosity. (*Tarek Ahmed, 2006*)

2.4 Porosity Measurements on core plugs:

From the definition of porosity, it is evident that the porosity of a sample of porous material can be determined by measuring any two of the three quantities: Bulk volume, pore volume or grain volume. The porosity of reservoir rock may be determined by - Core analysis - Well logging technique - Well testing the question of which source of porosity data is most reliable cannot be answered without reference to a specific interpretation problem. These techniques can all give correct porosity values under favorable conditions. The core analysis porosity determination has the advantage that no assumptions need to be made as to mineral composition, borehole effects, etc. However, since the volume of the core is less than the rock volume which is investigated by a logging device, porosity values derived from logs are frequently more accurate in heterogeneous reservoirs.

2.5 Bulk Volume Measurement:

Although the bulk volume may be computed from measurements of the dimensions of a uniformly shaped sample, the usual procedure utilizes the observation of the volume of fluid displaced by the sample. The fluid displaced by a sample can be observed either volumetrically

or gravimetrically. In either procedure it is necessary to prevent the fluid penetration into the pore space of the rock. This can be accomplished

(1) By coating the sample with paraffin or a similar substance

(2) By saturating the core with the fluid into which it is to be immersed or

(3) By using mercury.

Gravimetric determinations of bulk volume can be accomplished by observing the loss in weight of the sample when immersed in a fluid or by change in weight of a pycnometer with and without the core sample.

2.6 Grain Volume Measurement:

The grain volume of pore samples is sometimes calculated from sample weight and knowledge of average density. Formations of varying lithology and, hence, grain density limit applicability of this method. Boyle's law is often employed with helium as the gas to determine grain volume. The technique is fairly rapid, and is valid on clean and dry sample.

The measurement of the grain volume of a core sample may also be based on the loss in weight of a saturated sample plunged in a liquid.

Grain volume may be measured by crushing a dry and clean core sample. The volume of crushed sample is then determined by (either pycnometer or) immersing in a suitable liquid. *(Torsæter and M. Abtahi, 2003)*

2.7 Experiments

2.7.1 Porosity Determination by Liquid Saturating Method

Description:

The determination of the effective liquid porosity of a porous plug is the initial part of the measurement of capillary pressure using porous plate method in core laboratories. Before the capillary pressure is determined the volume of the saturating liquid (brine or oil) in the core must

be known. Thus, the effective liquid porosity of the core can be calculated in the beginning of capillary pressure measurement.

Procedure:

1. Weigh dry Berea plug Wdry, measure its diameter D, and length L, with calliper (1 core for each group).

2. Put the cores in the beaker inside a vacuum container, run vacuum pump about 1 hour.

3. Saturate the cores with 36 g/l NaCl brine, ϱbrine = 1.02g/cm3.

4. Weigh the saturated cores, Wsat.

Calculations and report:

1. Calculate the saturated brine weight, Wbrine = Wsat-Wdry.

2. Calculate the pore volume (saturated brine volume), Vp = Wsat/ ϱbrine.

3. Calculate effective porosity, φe = Vp/Vb

2.8 Saturation

Saturation is defined as that fraction, or percent, of the pore volume occupied by a particular fluid (oil, gas, or water). This property is expressed mathematically by the following relationship

$$\textbf{Fluid saturation} = \frac{\textbf{total volume of the fluid}}{\textbf{pore volume}} \quad \ldots\ldots\ldots\ldots (2.4)$$

Applying the above mathematical concept of saturation to each reservoir fluid gives

$$So = \frac{\textbf{volume of oil}}{\textbf{pore volume}} \quad \ldots\ldots\ldots (2.5)$$

$$S_g \frac{\textbf{volume of gas}}{\textbf{pore volume}} \quad \text{……. (2.6)}$$

$$Sw = \frac{\textbf{volume of water}}{\textbf{pore volume}} \quad \text{……. (2.7)}$$

Where:

So = oil saturation

S_g = gas saturation

S_w = water saturation

Thus, all saturation values are based on pore volume and not on the gross reservoir volume. The saturation of each individual phase ranges between zero to 100%. By definition, the sum of the saturations is 100%, therefore

Sg + So + Sw = 1 …… (2.8)

The fluids in most reservoirs are believed to have reached a state of equilibrium and, therefore, will have become separated according to their density, i.e., oil overlain by gas and underlain by water.

2.9 Critical oil saturation, Soc:

For the oil phase to flow, the saturation of the oil must exceed a certain value, which is termed critical oil saturation. At this particular saturation, the oil remains in the pores and, for all practical purposes, will not flow.

2.10 Residual oil saturation, Sor:

During the displacing process of the crude oil system from the porous media by water or gas injection (or encroachment), there will be some remaining oil left that is quantitatively characterized by a saturation value that is larger than the critical oil saturation. This saturation value is called the residual oil saturation, Sor. The term residual saturation is usually associated with the nonwetting phase when it is being displaced by a wetting phase.

2.11 Critical gas saturation, Sgc:

As the reservoir pressure declines below the bubble-point pressure, gas evolves from the oil phase and consequently the saturation of the gas increases as the reservoir pressure declines. The gas phase remains immobile until its saturation exceeds a certain saturation, called critical gas saturation, above which gas begins to move.

2.12 Critical water saturation, S_{wc}:

The critical water saturation, connate water saturation, and irreducible water saturation are extensively used interchangeably to define the maxi- mum water saturation at which the water phase will remain immobile.

2.13 CONTACT ANGLE AND WETTABILITY

2.13.1 Definitions:

When a liquid is brought into contact with a solid surface, the liquid either expand over the whole surface or form small drops on the surface. In the first case the liquid will wet the solid completely, whereas in the later case a contact angle $\Theta > 0$ will develop between the surface and the drop. When two immiscible fluids contact a solid surface, one of them tends to spread or adhere to it more so than the other.

2.13.2 Measurements on Core Samples:

In porous media the contact angle is determined indirectly. The methods are mainly based on measurements during displacement tests. But the problem is that no valid theory is developed for the relationship between displacement pressure and wetting preference.

2.13.3 The Amott Method:

The test developed by Amott seems to be most accepted and widely used test in the oil industry. In principle, a core sample is chosen and saturated with oil. The oil-saturated sample is then placed in an imbibition cell surrounded by water. The water is allowed to imbibe into the core sample displacing oil out of the sample until equilibrium is reached. The volume of water imbibed is measured.

The core sample is then removed and the remaining oil in the sample is forced down to residual saturation by displacement with water. This may be done either in a centrifuge or displaced with a pump in a sealed core holder. The volume of oil displaced may be measured directly or determined by weight measurements. The core, now saturated with water at residual oil saturation, is placed in an imbibition cell and surrounded by oil. The oil is allowed to imbible into the core displacing water out of the sample. The volume of water displaced is measured (equal to volume of oil imbibed). The core is removed from the cell after equilibrium is reached, and remaining water in the core is forced out by displacement in a centrifuge. The volume of water displaced is measured By recording all volumes produced, it is possible to calculate a wettability index WI

$$WI = \frac{Vo1}{Vo1+Vo2} - \frac{Vw1}{Vw1+Vw2} = rw - ro \quad \text{..... (2.9)}$$

Where:

VO1 = volume of oil produced during water imbibition

VO2 = volume of oil produced during water flooding

VW1 = volume of water produced during oil “imbibition”

VW2 = volume of water produced during oil flooding

rw = displacement-with-water-ratio

ro = displacement-with-oil-ratio.

The wettability index will be a number between –1.0 and 1.0

Where:

WI = 1.0 completely water wetting

WI = 0.0 neutral

WI = -1.0 completely oil wetting.

The test is a fully empirical test but is based on some theoretical reasoning. A drawback is that the tests are difficult to perform at reservoir pressure and temperature.

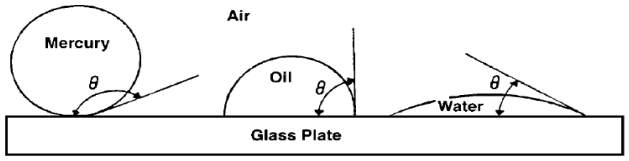

Fig (2-1): The Concept of Wettability (*Tarek Ahmed, 2006*)

2.14 CAPILLARY PRESSURE

2.14.1 Definitions:

When two immiscble fluids are in contact in the interstices of a porous medium, a discontinuity in pressure exists across the interface separating them. The difference in pressure Pc is called capillary pressure, which is pressure in the non-wetting phase minus the pressure in the wetting phase

$$P_c = P_{non\ wetting} - p_{wetting} \quad \text{……. (2.9)}$$

Thus, the capillary pressure may have either positive or negative values. For an oil-water, gas-water or gas-oil system, capillary pressure is defined as

$$P_c = P_o - p_w \quad \text{……. (2.10)}$$

$$P_c = P_g - p_w \quad \text{……... (2.11)}$$

$$P_c = P_g - P_o \quad \text{…….. (2.12)}$$

2.14.2 Experiments

2.14.3 Air/Brine Capillary Pressure at Ambient Conditions:

i. The plug samples were fully saturated in synthetic formation brine, the samples were moved onto air/brine capillary pressure and resistivity index analysis.

ii. Each porous plate was brine saturated by vacuum followed by flow through.

iii. Each sample was initially loaded onto a 0.5 bar rated porous plate in a capillary pressure cell. A diatomaceous earth (Kieselguhr) was used to enhance the capillary contact of the sample and the plate. Sample desaturation was achieved using humidified nitrogen gas at several different displacement pressures. Brine effluent from the samples was collected in a container outside the capillary pressure cell. The volume of brine displaced was monitored daily. When it remained stable over a period of three days, indicating that saturation equilibrium had been achieved in the core samples, the partially saturated plugs were removed from the cell and weighed.

iv. As the capillary pressure (Pc) increased, the plate was changed to be within the pressure rating. This system facilitates quicker equilibration.

v. Each sample was DE saturated at pressures of 1, 4,10,30,60,100 and 200 psig.

vi. The Air-Brine Capillary Pressure results are presented in tables and attached figures.

2.15 Leverett J-Function:

Capillary pressure data are obtained on small core samples that represent an extremely small part of the reservoir, and, therefore, it is necessary to combine all capillary data to classify a particular reservoir. The fact that the capillary pressure-saturation curves of nearly all naturally porous materials have many features in common has led to attempts to devise some general equation describing all such curves. Leverett (1941) approached the problem from the standpoint of dimensional analysis. Realizing that capillary pressure should depend on the porosity, interfacial tension, and mean pore radius, Leverett defined the dimensionless function of saturation, which he called the J-function, as

$$J = \frac{0.2166.Pc.\sqrt{(\frac{K}{\emptyset})}}{\sigma.cos\theta} \text{ ..... (2.13)}$$

Where:

J = Leverett capillary pressure function, dimensionless

Pc= Capillary pressure, psia

σ = Air-mercury interfacial tension

Θ = Air-mercury contact angle

K = peremebility

φ = porosity

2.16 PERMEABILITY

2.16.1 Definition

Permeability is a property of the porous medium and it is a measure of capacity of the medium to transmit fluids. Permeability is a tensor that in general is a function of pressure. Usually, the pressure dependence is neglected in reservoir calculations, but the variation with position can be pronounced. Very often the permeability varies by several magnitudes, and such heterogeneity will of course influence any oil recovery.

This rock characterization was first defined mathematically by Henry Darcy in 1856. In fact, the equation that defines permeability in terms of measurable quantities is called Darcy's Law. Darcy developed a fluid flow equation that has since become one of the standard mathematical tools of the petroleum engineer. If a horizontal linear flow of an incompressible fluid is established through a core sample of length L and a cross-section of area A, then the governing fluid flow equation is defined as

$$V = \frac{-K}{\mu}\left(\frac{dp}{dL}\right) \quad \text{..... (2.14)}$$

Where

v=apparent fluid flowing velocity, cm/sec

k = proportionality constant, or permeability, Darcy's

μ=viscosity of the flowing fluid, cp

dp/dL = pressure drop per unit length, atm/c

2.16.2 Effective permeability:

Is the ability of the porous material to conduct a fluid when its saturation is less than 100% of the pore space.

2.16.3 Relative permeability:

Is the ratio of the effective permeability of a given phase, say oil ko, in presence of other phases (water and/or gas), to the absolute permeability *k:*

$$K_{ro} = \frac{Ko}{k} \quad \text{..... (2.15)}$$

2.17 Well logging

Logging, electro logging or well logging means continuous recording of a physical parameter of the formation with depth.

Standard Logging

1. Formation Gamma Ray
2. Caliper (hole size)
3. Spontaneous potential log(SP)
4. Porosity logs:

I. Neutron Porosity
II. Density (Porosity)
III. Sonic

5. Resistivity logs

I. Shallow resistivity log
II. Deep resistivity log
III. Micro resistivity log

2.17.1 Gamma ray log:

The Gamma Ray log is a measurement of the formation's natural radioactivity. Gamma ray emission is produced by three radioactive series found in the Earth's crust.

- Potassium (K40)
- Uranium
- Thorium

It also known as shale log and reflect shale or clay content the advantage of GR log is that it works through the steel and cement walls of cased bore hole

Can calculate the shale voluom from GR log using this equation:

$$\mathbf{IGR} = \frac{\mathbf{GRlog - GRclean}}{\mathbf{GRshale - GRclean}} \quad \textbf{..... (2.16)}$$

$$\boldsymbol{Vsh} = \mathbf{0.33[2^{(2*IGR)} - 1.0]} \quad \textbf{..... (2.17)}$$

Where:

IGR = gamma ray index

GR_{log} = reading of gamma ray from log

GR_{clean} = clean sand stone

GR_{shale} = shale GR

Vsh = shale volume

The scale of GR log is (0-150)

2.17.2 Spontaneous Potential - SP

The SP log, like the natural gamma ray log is a recording of naturally occurring physical phenomena in the formations in a wellbore. The SP log is a recording versus depth of the difference between the electrical potential of a movable electrode in the borehole and the electrical potential of a fixed surface electrode.

The SP log has several oilfield applications:

1. Correlation
2. Identify the fresh / salt water interface
3. Qualitative indication of bed shaliness
4. Determination of formation water resistivity

Measures the electrical potential in the formation caused by the salinity difference between the drilling mud and the formation water and SP is generally an indicator of permeability. Shale must be present next to a permeable zone like a sand stone in order to have an SP but Limestone's normally do not have SP due to low permeability and high resistivity. The SP cannot be recorded in holes with nonconductive muds because such muds do not provide electrical continuity between the SP electrode and the formation, The SP can only be recorded in open hole because there must be ion movement between fluids to establish the spontaneous potential. If the resistivity's of the mud filtrate and the formation water are about equal, the SP deflections will be small and the curve rather featureless. The SP log measures the electrical potential in the formation. This is a relative measurement. The deflection on the SP log is measured from the shale to the sand and The amount of deflection that you see between the shale and the sand is a relative amount of deflection. The log analyst does not read the value of the SP log directly from the log. Rather, it is the difference between the shale reading and the sand reading.

2.17.3 Porosity logs

2.17.3.1 Density Logs:

Uses radioactive source to generate gamma rays, Gamma ray collides with electrons in formation, losing energy and Detector measures reduced intensity of gamma rays

By measuring the number of gamma rays and their energy levels at a given distance from the source, the electron density of the formation can be predicted

Response of density tools is a function of the formation's electron density, Electron density is a measure of bulk density and Bulk density is dependent upon:

a. Rock lithology
b. Formation porosity
c. Density and saturation of fluids in pore space

Porosity from Density Log:

$$\emptyset = \frac{\rho ma - \rho b}{\rho ma - \rho f} \quad \textbf{…….. (2.18)}$$

Where:

Φ = porosity

ρma = matrix density

ρb = Bulk density

ρf = fluid density

Factors Affecting Density Log Response

- Borehole and mud filtrate effects
- Shales and clays
- Hydrocarbons

2.17.3.2 Neutron Log:

Logging tool emits high energy neutrons into formation then Neutrons collide with nuclei of formation's atom and Neutrons lose energy (velocity) with each collision Most energy lost when colliding with a hydrogen atom nucleus, Neutrons are slowed sufficiently to be captured by nuclei Capturing nuclei become excited and emit gamma rays.

Depending on type of logging tool either gamma rays or neutrons emitted are captured Log records porosity based on neutrons captured by formation, if hydrogen is in pore space, porosity is related to the ratio of neutrons emitted to those counted

Neutron tools emit high energy neutrons from either a chemical source or a neutron generator device (minitron) and measure the response of these neutrons as they interact with the formation, or in many cases, the fluids within the formation. This measured response is affected by the quantity of neutrons at different energy levels and by the decay rate of the neutron population from one given energy level to another. A neutron interacts with the formation in a variety of ways after leaving the source; it is the aftermath of these interactions that is detected by the tool. Neutrons are approximately the same size as a hydrogen atom. When a neutron strikes hydrogen atom it will lose a large amount of energy. If it strikes a larger atom, it will not lose as much energy. If there are lots of hydrogen atoms, there will be less neutrons which return to the detector. When less neutrons are detected, it is an indication of larger porosity.

2.17.3.3 Neutron Porosity:

Applications:

1. Porosity analysis

In clean formations that have pores filled with water or oil, the neutron measurement can be used to derive liquid-filled porosity. This is done using the hydrogen index (HI) concept.

2. Gas detection

Gas zones (i.e. not liquid-filled) can often be identified by comparing the neutron porosity log with another porosity log, such as a density or sonic log. (Neutron porosity reads much lower than Density and Sonic porosity in gas zones.)

3. Lithology

By combining the density/neutron tool information, it is possible to get a good estimate of likely formation lithology.

2.17.3.4 Acoustic log (sonic):

Acoustic tools measure the speed of sound waves in subsurface formation. Tool usually consists of one sound transmitter (above) and two receivers (below) Sound is generated, travels through formation Elapsed time between sound wave at receiver 1 vs. receiver 2 is dependent upon density of medium through which the sound travelled.

$$\Phi s = \frac{tlog - tma}{tf - tma} \quad \text{..... (2.19)}$$

Where:

Φs = porosity from sonic

T_{log} = reading of travel time from log

T_{ma} = travel time of matrix

T_f = travel time of fluid

Factors Affecting Sonic Log Response

• Unconsolidated formations (Compaction Correction Factor ~ 1.6 for unconsolidated sand).

• Naturally fractured formations

• Hydrocarbons (especially gas)

• Rugose salt sections

Applications of sonic log

1. Indicating lithology
2. Determining integrated travel time
3. Detecting fractures and evaluating secondary recovery porosity
4. Evaluating cement bonds between casing and formation

2.17.4 Resistivity log:

Resistivity log measures the ability of rock to conduct electrical current and are sealed in units of ohm-meters, the resistivity of a rock will depend on the conductivity of the fluids saturating the porous volume. Hydrocarbons (oil or gas) have a very high resistivity. Formation water has a resistivity value that changes depending on the salinity and temperature of the water. Resistivity profile is the radial distribution of resistivity resulting from the invasion of fluids having different conductivity than the formation fluids

2.17.4.1 Two types of log available:

i. Induction logs: run in nonconductive or low- conductivity muds
ii. Laterologs: run in highly conductive muds (salt based)

CHAPTER3

RELATIVE PERMEABILITY, CAPILLARY PRESSURE AND WELL LOGGING ANALYSIS

3.1 Relative permeability:

Relative permeability is the ratio of the effective permeability of a given phase, say oil ko, in presence of other phases (water and/or gas), to the absolute permeability *k*.

$$\mathbf{K_{ro} = \frac{ko}{k}} \quad \textbf{……. (3.1)}$$

Where:

K_{ro} = relative permeability of oil

K_o = permeability of oil

K = absolute permeability

When a wetting and a nonwetting phase flow together in a reservoir rock, each phase follows separate and distinct paths. The distribution of the two phases according to their wetting characteristics results in characteristic wetting and nonwetting phase relative permeabilities. Since the wetting phase occupies the smaller pore openings at small saturations, and these pore openings do not contribute materially to flow, it follows that the presence of small wetting phase saturation will affect the nonwetting phase permeability only to a limited extent. Since the nonwetting phase occupies the central or larger pore openings that contribute materially to fluid flow through the reservoir, however, small nonwetting phase saturation will drastically reduce the wetting phase permeability.

Figure (3-1) presents a typical set of relative permeability curves for a water-oil system with the water being considered the wetting phase and shows the following four distinct and significant observations:

• Observation 1:

The wetting phase relative permeability shows that a small saturation of the nonwetting phase will drastically reduce the relative permeability of the wetting phase. The reason for this is that the nonwetting phase occupies the larger pore spaces, and it is in these large pore spaces that flow occurs with the least difficulty.

• Observation 2:

The nonwetting phase relative permeability curve shows that the nonwetting phase begins to flow at the relatively low saturation of the nonwetting phase. The saturation of the oil at this point is called *critical oil saturation* Soc.

• Observation 3:

The wetting phase relative permeability curve shows that the wetting phase will cease to flow at a relatively large saturation. This is because the wetting phase preferentially occupies the smaller pore spaces, where capillary forces are the greatest. The saturation of the water at this point is referred to as the irreducible water saturation Swir or connate-water saturation S_{wi}both terms are used interchangeably.

• Observation 4:

The nonwetting phase relative permeability curve shows that, at the lower saturations of the wetting phase, changes in the wetting phase saturation have only a small effect on the magnitude

of the nonwetting phase relative permeability curve. The reason for the phenomenon at Point 4 is that at the low saturations, the wetting phase fluid occupies

the small pore spaces that do not contribute materially to flow, and therefore changing the saturation, in these small pore spaces has a relatively small effect on the flow of the nonwetting phase. This process could have been visualized in reverse just as well. It should be noted that this example portrays oil as nonwetting and water as wetting. The curve shapes shown are typical for wetting and nonwetting phases and may be mentally reversed to visualize the behavior of an oil-wet system. Note also that the total permeability to both phases, krw + kro, is less than 1, in regions B and C.

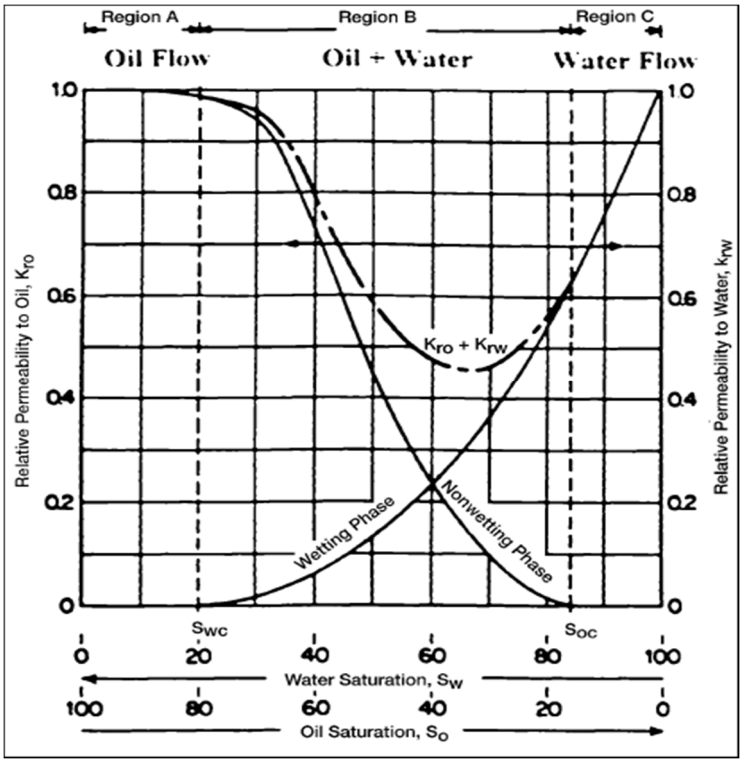

Fig (3 - 1): Relative Permeability Curves (Tarek Ahmed, 2006)

3.2 Two-Phase Relative Permeability Correlations

In many cases, relative permeability data on actual samples from the reservoir under study may not be available, in which case it is necessary to obtain the desired relative permeability data in some other manner. Field relative permeability data can usually be calculated. The field data are unavailable for future production, however, and some substitute must be devised. Several methods have been developed for calculating relative permeability relationships. Various parameters have been used to calculate the relative permeability relationships, including:

1. Residual and initial saturations
2. Capillary pressure data

In addition, most of the proposed correlations use the effective phase

Saturation as a correlating parameter. The effective phase saturation is defined by the following set of relationships:

$$S_o^* = \frac{So}{1-Swc} \quad \text{.....(3.2)}$$

$$S_w^* = \frac{Sw-Swc}{1-Swc} \quad \text{..... (3.3)}$$

$$S_g^* = \frac{Sgc}{1-Swc} \quad \text{..... (3.4)}$$

Where:

S_o^*, S_{g*}, S_w^* = effective oil , gas , and water saturation , respectively

S_o , S_g , S_w = oil , gas ,and water saturation , respectively

3.3 Wyllie and Gardner Correlation

Wyllie and Gardner (1958) observed that, in some rocks, the relationship between the reciprocal capillary pressure squared ($1/Pc^2$) and the effective water saturation s_w^* is over a wide range of saturation. Honapour et al. (1988) conveniently tabulated Wyllie and Gardner correlation as shown below:

Unconsolidated sand, well sorted:

$$K_{ro} = (1- S_w^*) \quad \text{..... (3.5)}$$

$$K_{rw} = (S_w^*)^3 \quad \text{..... (3.6)}$$

Unconsolidated sand, poorly sorted:

$$K_{ro} = (1-s_{w*})^2 (1-s_{w*}^{1.5}) \quad \text{..... (3.7)}$$

$$K_{rw} = (S_{o*})^{3.5} \quad \text{..... (3.8)}$$

Cemented sandstone:

$$K_{ro} = (1-s_{w*})^2 (1-s_{w*}^2) \quad \text{..... (3.9)}$$

$$K_{ro} = (s_{o*})^4 \quad \text{..... (3.10)}$$

3.4 Torcaso and Wyllie Correlation

Torcaso and Wyllie (1958) developed a simple expression to determine

The relative permeability of the oil phase in a gas-oil system. The expression

Permits the calculation of kro from the measurements of krg. The equation has the following form:

$$k_{ro} = k_{rg} \frac{(So*)4}{(1-So*)2(1-(So*)2)} \quad \text{..... (3.11)}$$

3.5 Corey's Method

Corey (1954) proposed a simple mathematical expression for generating the relative permeability data of the gas-oil system. The approximation is good for drainage processes, i.e., gas-displacing oil.

$$K_{ro} = (1-s_{g*})^4 \quad \text{..... (3.12)}$$

$$K_{rg} = (s_g^*)\,(2 - s_{g*}) \quad \text{..... (3.13)}$$

3.6 Capillary Pressure Analysis:

When two immiscible fluids are in contact, there will be force act on the interface between them and this force either terms surface tension if the the two immiscible fluids are gas and liquid or terms interfacial tension if the contact between two liquids and the combination of these forces is called capillary force . The discontinuity in pressure between two immiscible fluids are in contact depends upon the curvature of interface separating the fluids and this pressure difference is called capillary pressure (Tarek Ahmed, 2004).

3.7 Determination of capillary pressure from lab

Capillary pressure relationships normally are obtained in the lab by First saturating the core with the wetting phase then the core is Placed in a chamber , subjected to pressure and invaded by Nonwetting phase .this is done in steps with the pressure and volume Of wetting fluid displaced noted at each step . The pressure required to first causes any displacement from them.

Three methods are generally used for determination of capillary data on rock samples (O. Torsæter M. Abtahi , 2011):

- Purcell's method /mercury injection method

- Restored state method
- Centrifuge method

The analysis of capillary pressure data that measured at special core analysis laboratory include:

1. Plotting the water saturation versus capillary pressure which represents the data obtained at laboratory conditions.
2. Converting the laboratory condition data into reservoir condition data using the following equation:

$$\mathbf{Pc_{(res)} = Pc_{(lab)} \frac{(\sigma \cos \theta) res}{(\sigma \cos \theta) lab}} \quad \text{..... (3.14)}$$

Where:

$\mathbf{Pc_{(res)}}$ = reservoir Capillary pressure, psia

$\mathbf{Pc_{(lab)}}$ **= lab** capillary pressure

$(\sigma \cos \theta) res$ = oil-water interfacial tension and oil-water contact angle

$(\sigma \cos \theta) lab$ = Air-mercury interfacial tension and Air-mercury contact angle

K = peremeability

3. Converting all capillary pressure data to a universal curve using Leverett J_Function using the equation below:

$$\mathbf{J(Sw) = \frac{31.62\ Pc}{\sigma \cos \theta} \sqrt{\frac{k}{\Phi}}} \quad \text{..... (3.15)}$$

J = Leverett capillary pressure function, dimensionless

Pc= Capillary pressure, psia

σ = Air-mercury interfacial tension

Θ = Air-mercury contact angle

K = peremebility

φ = porosity

4. Calculate and plot the water saturation versus depth of the reservoir.

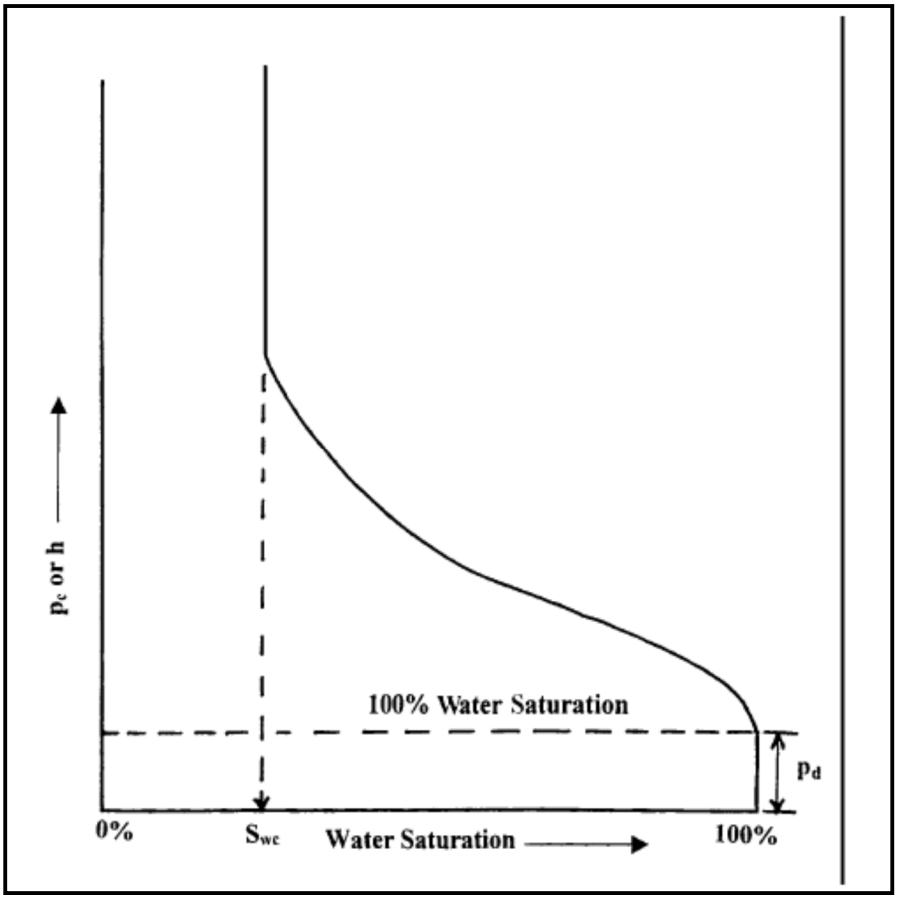

Figure (3-2): capillary pressure curve (Tarek Ahmed, 2006)

3.8 Well logging

Is moving a tool string at a certain logging speed and recorded the data at certain depth.

We will use interactive petrophysicis software (IP) to measure the reservoir rock and fluid properties

3.9 petrophysicis software (IP)

Interactive Petrophysics was developed by a petrophysicist, for petrophysicists, so they can work as they have always wanted to work. The software is different by design – portable, quick and versatile. It is an easy-to-use log analysis tool, ideal for both geologists and petrophysicists. A geologist can use it to make a swift quality check of his log data, but equally an experienced petrophysicist can use it for multi-zone, multi-well petrophysical field analyses.

IP is PC-based and therefore portable. It can be taken offshore, into clients' offices and even home. IP enhances efficiency, productivity and confidence in log analysis. It offers a unique and advanced graphical interpretation program designed and developed by petrophysicists. IP's speed and interactivity means that data can be zoned and applied using different methodologies graphically. Using only the mouse, you can pick parameters from cross plots, histograms and log plots. IP instantaneously recomputes and displays the results when parameters are changed.

The heart of IP is its graphical interpretation engine. This allows the user to perform a fast and sophisticated multi-zone interpretation using only the mouse, adjusting parameters on log plots, crossplots and histograms.

The standard deterministic analysis is done using three modules:

I. Clay Volume
II. Porosity and Water Saturation
III. Cutoff and Summation.

The Clay Volume module allows multiple clay indicators to be combined. Once the Clay Volumes have been determined the Porosity and Water Saturation module is run. This module uses the same intuitive interactive graphics.

3.9.1 Porosities can be calculated using several different methods:

1. Neutron / Density
2. Neutron / Sonic
3. Density
4. Sonic
5. Neutron.

3.9.2 Water Saturations are calculated using any standard method:

1. Archie
2. Simandoux
3. Indonesian
4. Dual Water
5. Juhasz
6. Waxman-Smits.

Hydrocarbon corrections are made using iterative techniques. A simple (optional) mineral analysis can be performed using the Rho Matrix / U Matrix / DT Matrix cross plot technique. Clay type distributions using the Thomas-Strieber technique can be made. This allows laminated shaley sands to be analyzed.

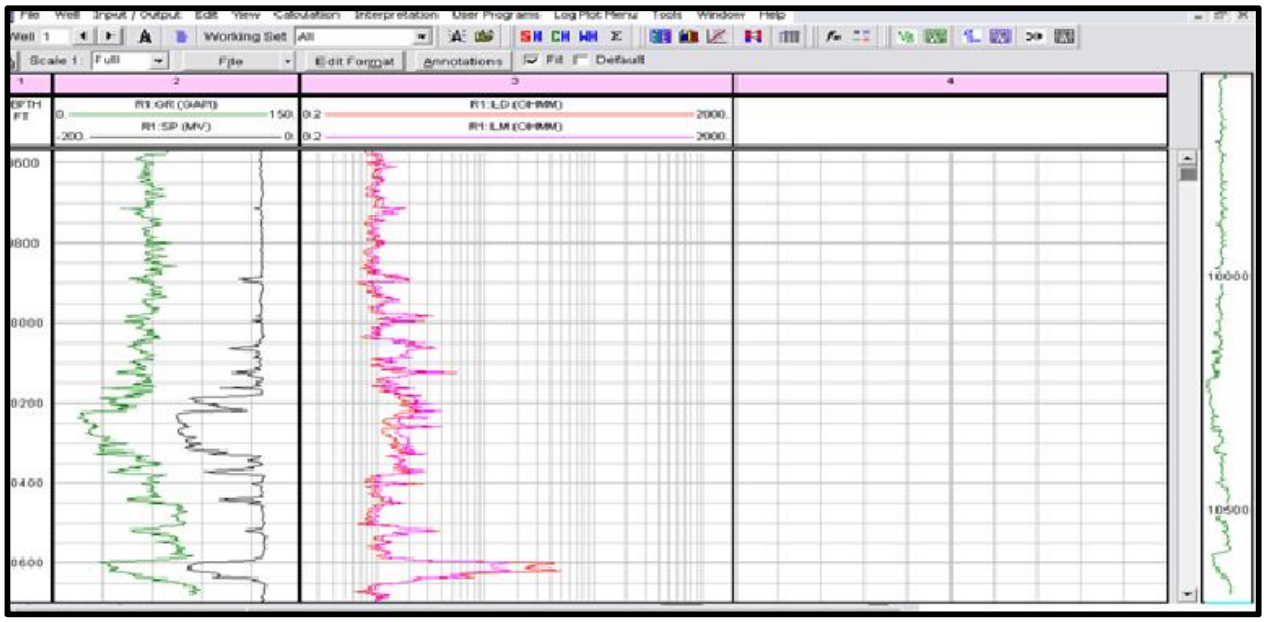

Fig (3-3): interactive pertrophysics software (Phil Davidson, 2009)

CHAPTER 4

RESULTS AND DISCUSSIONS

There are fifteen samples for two wells from **Bentiu Formation, Muglad Basin, Sudan** were available for this study. Seven samples are for Relative permeability laboratory data, eight samples are capillary pressure laboratory data and well logging data from three wells. Every sample was subjected to study and the final results were obtained as evaluation for bentiu formation.

4.1 Relative permeability:

The effective permeability of any reservoir fluid is a function of the reservoir fluid saturation and the wetting characteristics of the formation. Effective permeabilities are normally measured directly in the laboratory on small core plugs. Owing to many possible combinations of saturation for a single medium, however, laboratory data are usually summarized and reported as relative permeability.

4.2 Available Core Data:

The selected samples for this study were taken from bentiu Formation in Sudan. The objective of this analysis is to generate average oil – water relative permeability curve to represent the system subjected to the study. Tables below show these data.

4.2.1 Available data for South Annajma well 7:

SAMPLE (3S)

POROSITY(%) : 26.9
Swi = 44.3 (% PS)
Sor = 32.4 (% PS)
Ko @ Swi = 890 mD
Kw @ Sor = 124 mD

SAMPLE (10S)

POROSITY(%) : 26.4
Swi = 31.6 (% PS)
Sor = 23.3 (% PS)
Ko @ Swi = 612 mD
Kw @ Sor = 115 mD

Brine Saturation (% Pore Space)	kro	krw
44.3	1	-
50.3	0.212	0.029
53.5	0.1	0.04
55.7	0.066	0.05
57.7	0.04	0.061
59.7	0.026	0.07
61.5	0.016	0.083
63.1	0.009	0.096
64.4	0.006	0.107
65.6	0.004	0.119
67.6	-	0.14

Table (4-1): Sample 3S (depth 2031.9m)

Brine Saturation (% Pore Space)	**kro**	**krw**
31.6	1	-
47.4	0.405	0.019
51	0.31	0.03
54.6	0.234	0.043
57.6	0.183	0.056
60.3	0.151	0.069
62.8	0.118	0.083
65	0.094	0.099
66.8	0.073	0.112
68.6	0.058	0.128
70.3	0.04	0.135
71.6	0.026	0.146
74	0.01	0.168
75.6	0.005	0.183
76.7	-	0.188

Table (4-2): Sample 10S (depth 2167.4m)

SAMPLE 19S

SAMPLE 29S

POROSITY(%) : 23.2
Sor = 26.6 (% PS)
Swi = 35.4 (% PS)
Ko @ Swi = 319 mD
Kw @ Sor = 25 mD

Brine Saturation (% Pore Space)	kro	krw
35.4	1	-
48.5	0.27	0.01
55.2	0.12	0.02
62.7	0.043	0.042
64.9	0.028	0.049
66.5	0.02	0.055
68.4	0.012	0.061
69.6	0.008	0.065
70.6	0.005	0.069
71.3	0.004	0.071
72.4	0.002	0.076
73.4	-	0.078

Table (4-3): Sample 19S (depth 2249.3m)

POROSITY(%) : 19.3
Sor = 30.7 (% PS)
Swi = 29.5 (% PS)
Ko @ Swi = 350 mD
Kw @ Sor = 59.6 mD

Brine Saturation (% Pore Space)	kro	krw
29.54	1	-
46.95	0.316	0.034
51.86	0.21	0.056
55.79	0.147	0.076
59.72	0.09	0.098
63.65	0.049	0.125
65.61	0.031	0.14
67.58	0.015	0.152
68.25	0.01	0.159
69.3	-	0.17

Table (4-4): Sample 29S (depth 2461.6m)

4.2.2 Available data for South Annajma well 17:

SAMPLE 3

SAMPLE7

POROSITY(%) : 25.6
Ko @ Swi = 159 mD
Kw @ Sor = 9.66 mD
ka = 222 MD
Swi = 42.7 (% PS)
Sor = 29 (% PS)

POROSITY(%) : 24.9
Ko @ Swi = 215 mD
Kw @ Sor = 10.2 mD
ka = 321 mD
Swi = 40.3 (% PS)
Sor = 20.4 (% PS)

sw %	kro	krw
42.68	1	-
55.2	0.247	0.018
59.9	0.092	0.028
62	0.052	0.033
63.4	0.03	0.035
64.1	0.019	0.038
64.8	0.013	0.04
65.5	0.009	0.041
66.2	0.005	0.044
66.9	0.002	0.047
67.5	0.001	0.048
68.5	0.001	0.052
69.9	0.001	0.057
71	-	0.061

Table (4-5): Sample 3 (depth 1125m)

Sw%	kro	krw
40.27	1	-
50.6	0.347	0.018
57	0.182	0.03
64.5	0.058	0.039
66.8	0.031	0.04
68.4	0.022	0.04
69.5	0.015	0.041
70.3	0.012	0.042
71.2	0.008	0.042
72.1	0.007	0.042
73	0.005	0.043
74.8	0.003	0.044
76.1	0.001	0.043
77.9	0	0.046
79.57	-	0.047

Table (4-6): Sample 7 (depth 1174.4m)

POROSITY(%) : 26.2
Ko @ Swi = 755 mD
Kw @ Sor = 69.2 mD
ka = 1104 MD
Swi = 32.6 (% PS)
Sor = 23.2 (% PS)

sw%	kro	krw
32.6	1	-
46.4	0.356	0.017
58.5	0.116	0.037
62.5	0.069	0.047
64.2	0.054	0.053
65.4	0.046	0.055
66.2	0.037	0.057
67.4	0.032	0.06
68.8	0.025	0.065
70.6	0.018	0.071
74.3	0.005	0.083
76.8	-	0.092

Table (4-7): Sample 9 (depth 1181.6m)

4.3 Normalizing and Averaging Relative Permeability Data:

Usually the results of relative permeability tests on different core samples vary. Therefore, it is necessary to average the relative permeability data. The relative permeability curves should first be normalized to remove the effect of different initial water and critical oil saturations. The normalization process goes through the following steps:

4.3.1 Displaying Reported Results:

The results were plotted on two different scales linear and semi-log scales. On linear scale, a good test is normally depicted by K_{rw} curve concaving upward. Any deviation from this is considered an error and requires refinement. On semi-log scale both curves concave downward. Figures (4-1) through (4-8) show the relationship between S_w Vs. K_r on both linear and semi-log scales.

South Annajma well 7

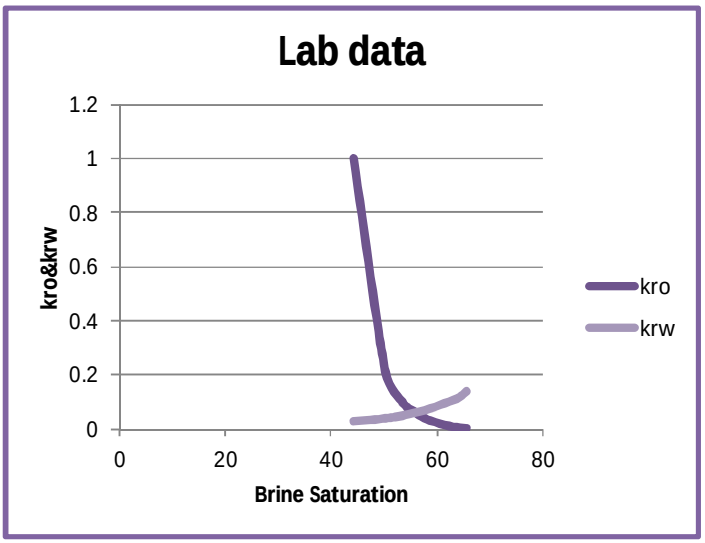

Fig (4-1): K_r VS. S_w for Sample3S

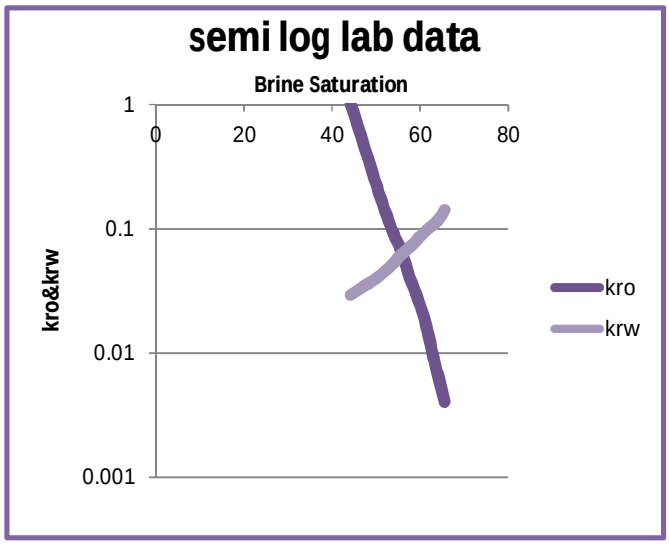

Fig (4-2): Semi log plot of Kr VS Sw for Sample (3S)

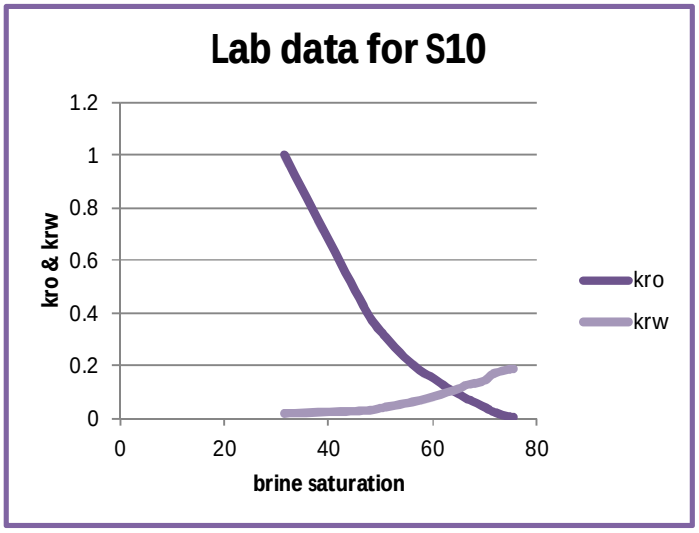

Fig (4-3): K_r Vs. S_w for Sample10S

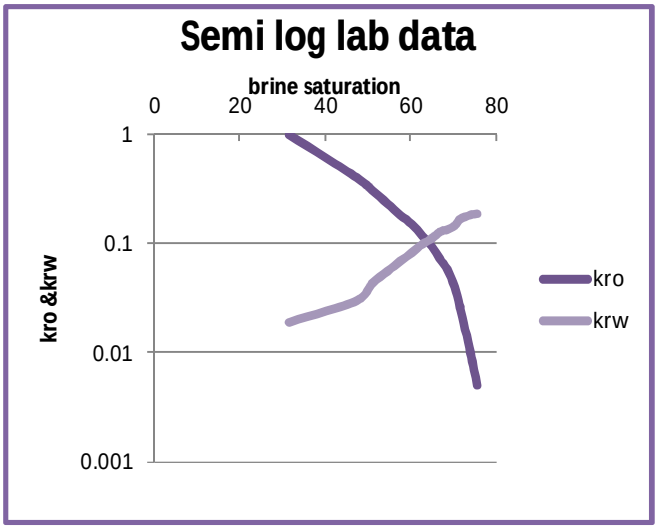

Fig (4-4): Semi log plot of Kr VS Sw for Sample (10S)

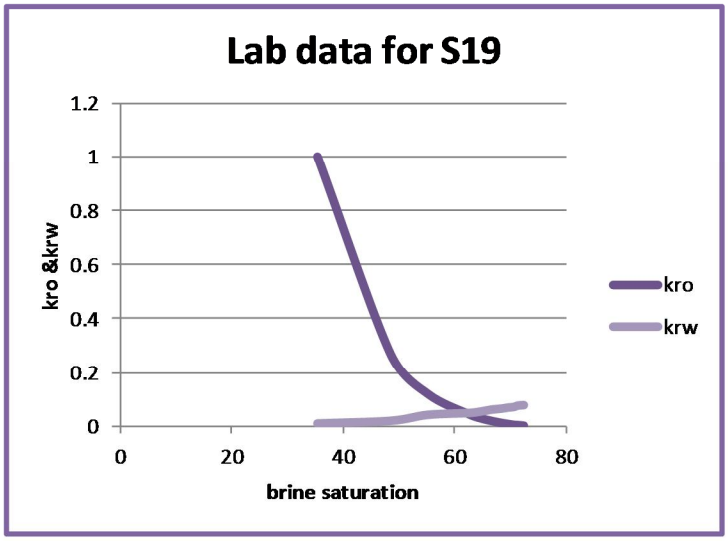

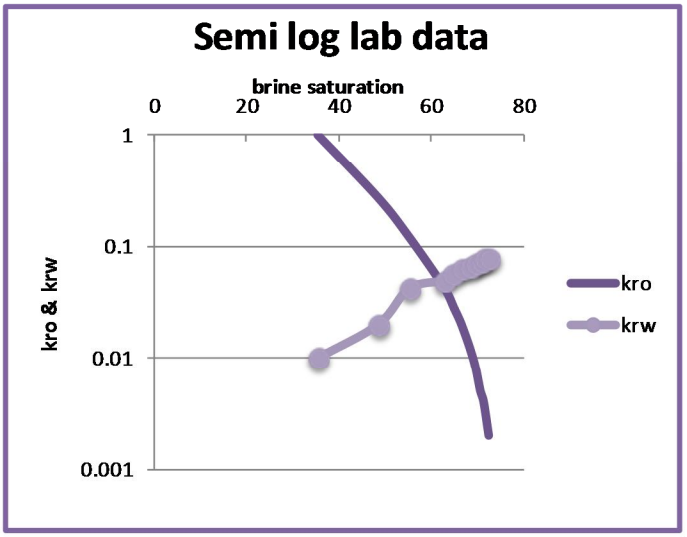

Fig (4-5): K_r Vs. S_w for Sample19S

Fig (4-6): Semi log plot of Kr VS Sw for Sample (19S)

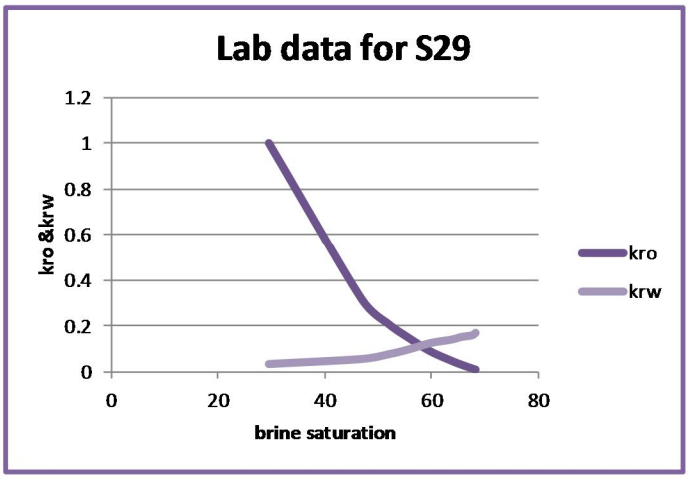

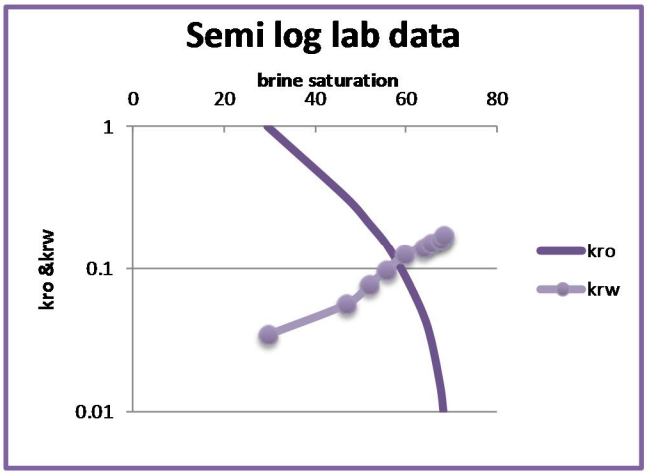

Fig (4-7): K_r Vs. S_w for Sample29S

Fig (4-8): Semi log plot of Kr VS Sw for Sample (29S)

South Annajma well 17

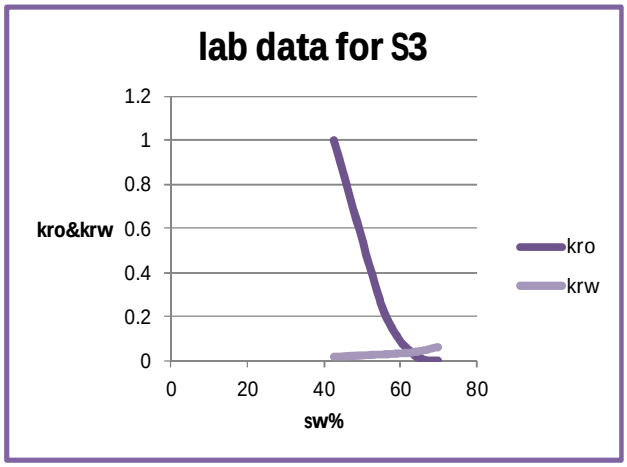

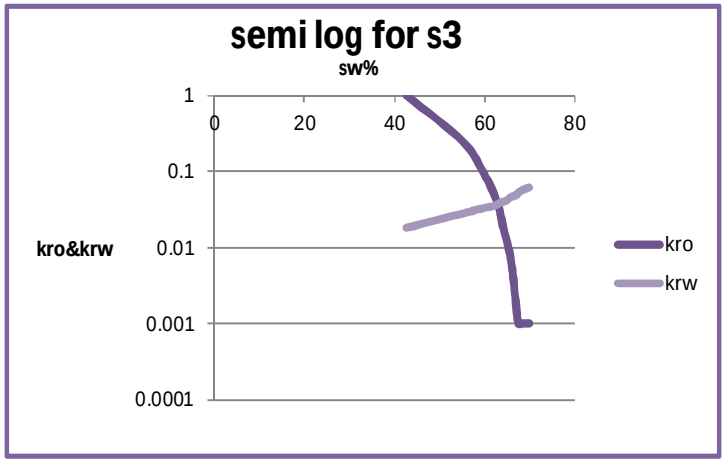

Fig (4-9): K_r Vs. S_w for Sample3

Fig (4-10): Semi log plot of Kr VS Sw for Sample (3)

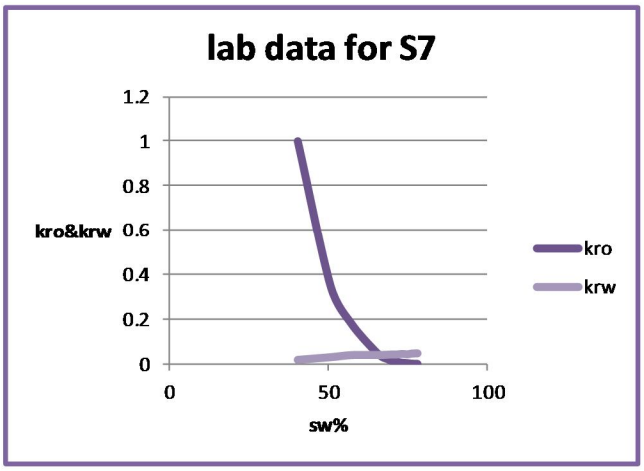

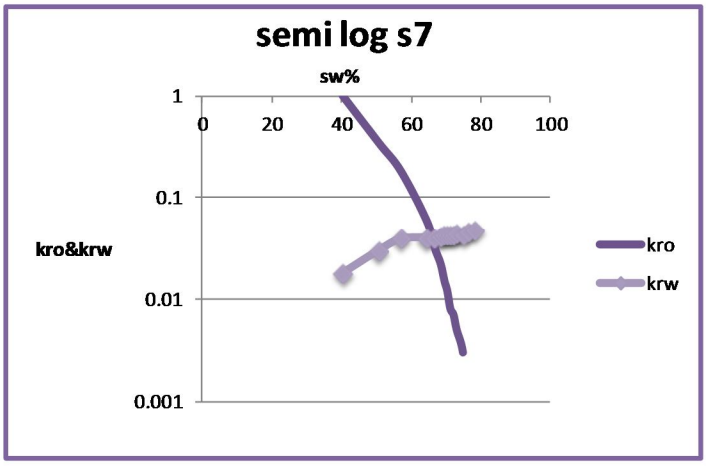

Fig (4-11): K_r Vs. S_w for Sample7

Fig (4-12): Semi log plot of Kr VS Sw for Sample7

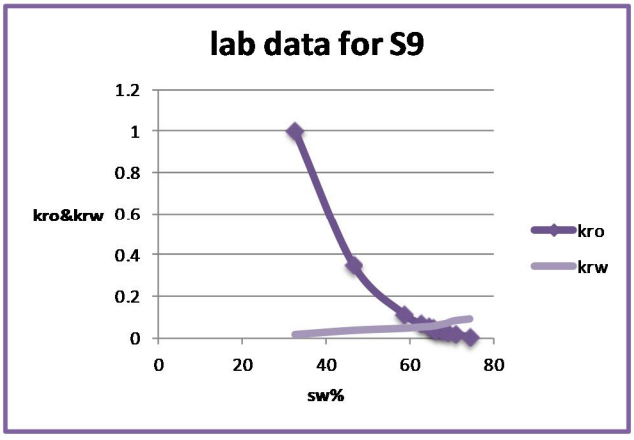

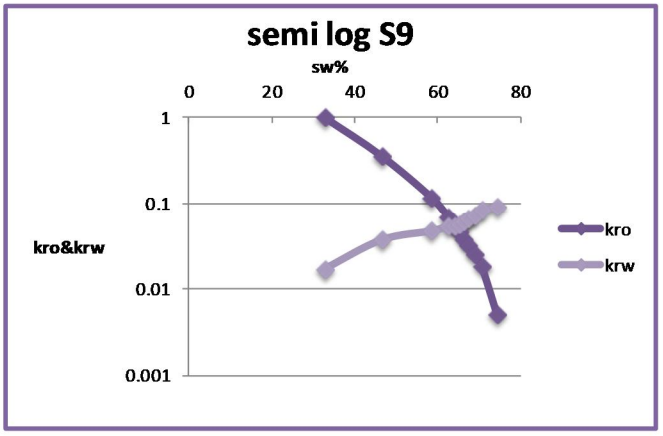

Fig (4-13): K_r Vs. S_w for Sample9

Fig (4-14): Semi log plot of Kr VS Sw for Sample9

4.3.2 Estimating True Residual Oil Saturation From Analysis of K_{ro} Curve :

Normalizing K_{ro} curves using different assumed values of S_{or} and noting which value produces a straight line on log-log plot of K_{ro} versus normalized oil saturation (So*) calculated using the following equation:

$$So* = \frac{1-Sw-Sor}{1-Swi-Sor} \quad \text{..... (4.1)}$$

Where:

S_o^* = normalized oil saturation

S_w = water saturation

S_{wi} = initial water saturation

S_{or} = residual oil saturation

Where No is the slope of true Sor line

Tables below show the true residual oil saturation for well (7) and well (17):

For well (7):

Sample (3S)

		So*		
sw	**kro**	**so*1=0.3**	**so*lab=0.324**	**so*3=0.33**
0.443	1	1.000	1.000	1.000
0.503	0.212	0.767	0.742	0.736
0.535	0.1	0.642	0.605	0.595
0.557	0.066	0.556	0.511	0.498
0.577	0.04	0.479	0.425	0.410
0.597	0.026	0.401	0.339	0.322
0.615	0.016	0.331	0.262	0.242
0.631	0.009	0.268	0.193	0.172
0.644	0.006	0.218	0.137	0.115
0.656	0.004	0.171	0.086	0.062
0.676	-			

Table (4-8): True S_{or} for Sample 3S

Sample (10S)

		So*		
sw	**kro**	**so*1=0.2**	**so*lab=0.233**	**so*3=0.24**
0.316	1	1.000	1.000	1.000
0.474	0.405	0.674	0.650	0.644
0.51	0.31	0.599	0.570	0.563
0.546	0.234	0.525	0.490	0.482
0.576	0.183	0.463	0.424	0.414
0.603	0.151	0.407	0.364	0.354
0.628	0.118	0.355	0.308	0.297
0.65	0.094	0.310	0.259	0.248
0.668	0.073	0.273	0.220	0.207
0.686	0.058	0.236	0.180	0.167
0.703	0.04	0.200	0.142	0.128
0.716	0.026	0.174	0.113	0.099
0.74	0.01	0.124	0.060	0.045

0.756	0.005	0.091	0.024	0.009
0.767	-	0.068	-	-

Table (4-9): True S_{or} for Sample 10S

Sample 19S

			So*	
sw	**Kro**	**so*1=0.25**	**so*lab=0.266**	**so*3=0.28**
0.354	1	1.000	1.000	1.000
0.485	0.27	0.669	0.655	0.642
0.552	0.12	0.500	0.479	0.459
0.627	0.043	0.311	0.282	0.254
0.649	0.028	0.255	0.224	0.194
0.665	0.02	0.215	0.182	0.150
0.684	0.012	0.167	0.132	0.098
0.696	0.008	0.136	0.100	0.066
0.706	0.005	0.111	0.074	0.038
0.713	0.004	0.093	0.055	0.019
0.724	0.002	0.066	0.026	
0.734	-	0.040		

Table (4-10): True S_{or} for Sample 19S

Sample 29S

			So*	
sw	**kro**	**so*1=0.3**	**so*lab=0.307**	**so*3=0.32**
0.295	1.000	1.000	1.000	1.000
0.470	0.316	0.570	0.562	0.547
0.519	0.210	0.448	0.439	0.420
0.558	0.147	0.351	0.340	0.317
0.597	0.090	0.254	0.241	0.215
0.637	0.049	0.157	0.142	0.113
0.656	0.031	0.109	0.093	0.062
0.676	0.015	0.060	0.043	0.011
0.683	0.010	0.043	0.026	
0.693	-	0.017		

Table (4-11): True S_{or} for Sample 29S

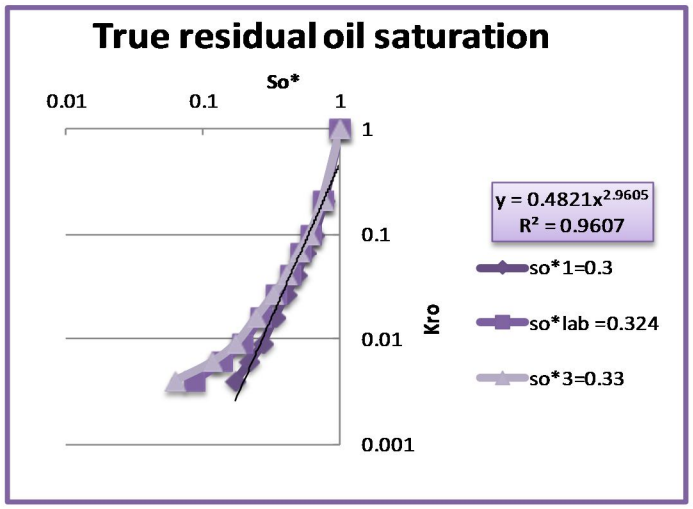

Fig (4-15): logarithmic scale of Kro Vs. So* for 3S

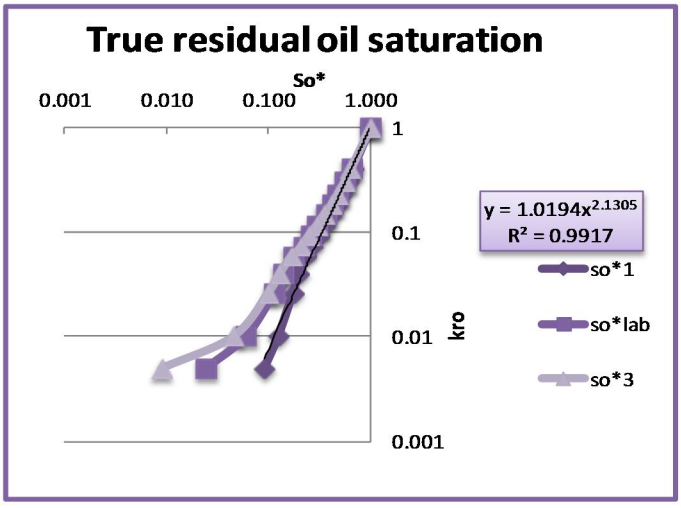

Fig (4-16): logarithmic scale Kro Vs. So* for 10S

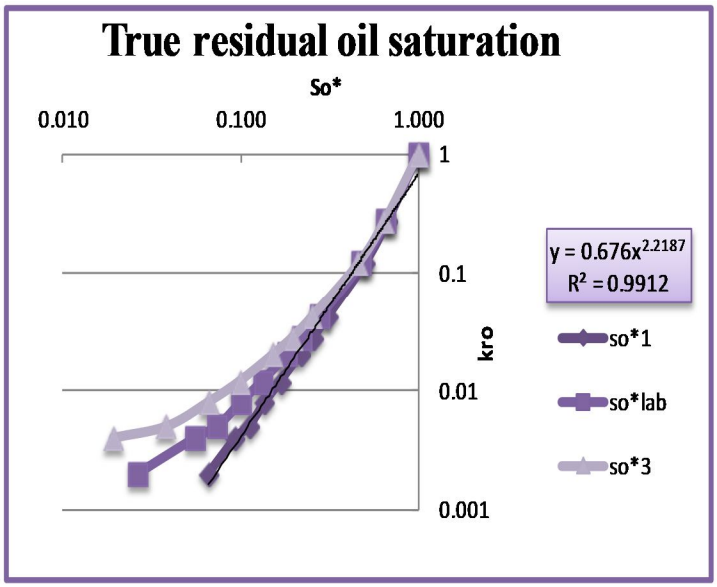

Fig (4-17): logarithmic scale of Kro Vs. So* for 19S

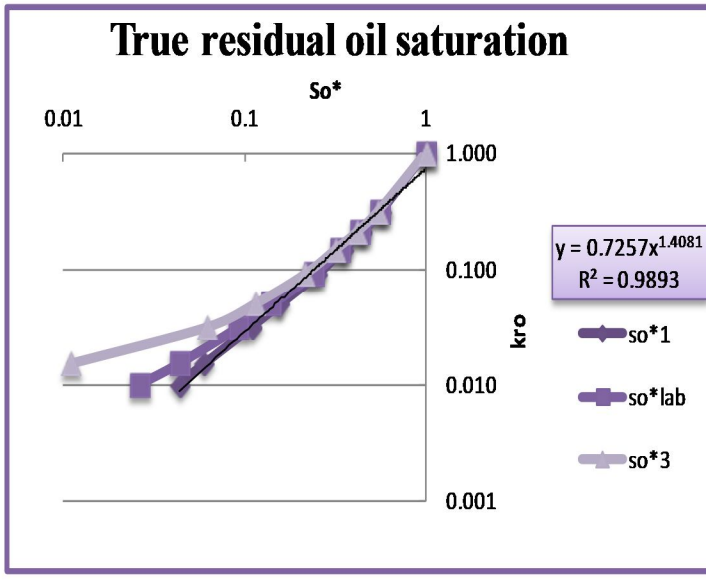

Fig (4-18): logarithmic scale Kro Vs. So* for 29S

For well 17:

Sample 3

		So*		
sw	kro	So*1=0.28	So*lab=0.29	So*3=0.3
0.427	1.000	1.000	1.000	1.000
0.552	0.247	0.573	0.558	0.542
0.599	0.092	0.413	0.392	0.370
0.620	0.052	0.341	0.318	0.293
0.634	0.030	0.293	0.268	0.242
0.641	0.019	0.269	0.244	0.216
0.648	0.013	0.246	0.219	0.190
0.655	0.009	0.222	0.194	0.165
0.662	0.005	0.198	0.169	0.139
0.669	0.002	0.174	0.145	0.113
0.675	0.001	0.153	0.124	0.092
0.685	0.001	0.119	0.088	0.055
0.699	0.001	0.072	0.039	0.004
0.710	-	0.034	0.000	-0.037

Table (4-12): True S_{or} for Sample 3

Sample 7

		So*		
Sw	**kro**	**So*1=0.2**	**So*lab=0.204**	**So*3= 0.21**
0.403	1.000	1.000	1.000	1.000
0.506	0.347	0.740	0.737	0.733
0.570	0.182	0.579	0.575	0.568
0.645	0.058	0.390	0.384	0.374
0.668	0.031	0.332	0.325	0.315
0.684	0.022	0.292	0.285	0.274
0.695	0.015	0.264	0.257	0.245
0.703	0.012	0.244	0.236	0.225
0.712	0.008	0.221	0.214	0.201
0.721	0.007	0.199	0.191	0.178
0.730	0.005	0.176	0.168	0.155
0.748	0.003	0.131	0.122	0.108

0.761	0.001	0.098	0.089	0.075
0.779	0.000	0.053	0.043	0.028
0.796	-	0.011	0.001	-0.015

Table (4-13): True S_{or} for Sample 7

Sample 9

		So*		
sw	**kro**	**So*1 = 0.2**	**so*lab = 0.232**	**so*3 = 0.24**
0.33	1.00	1.00	1.00	1.00
0.46	0.36	0.71	0.69	0.68
0.59	0.12	0.45	0.41	0.40
0.63	0.07	0.37	0.32	0.31
0.64	0.05	0.33	0.29	0.27
0.65	0.05	0.31	0.26	0.24
0.66	0.04	0.29	0.24	0.23
0.67	0.03	0.27	0.21	0.20
0.69	0.03	0.24	0.18	0.17
0.71	0.02	0.20	0.14	0.12
0.74	0.01	0.12	0.06	0.04
0.77	-	0.07	0.00	-0.02

Table (4-14): True S_{or} for Sample 9

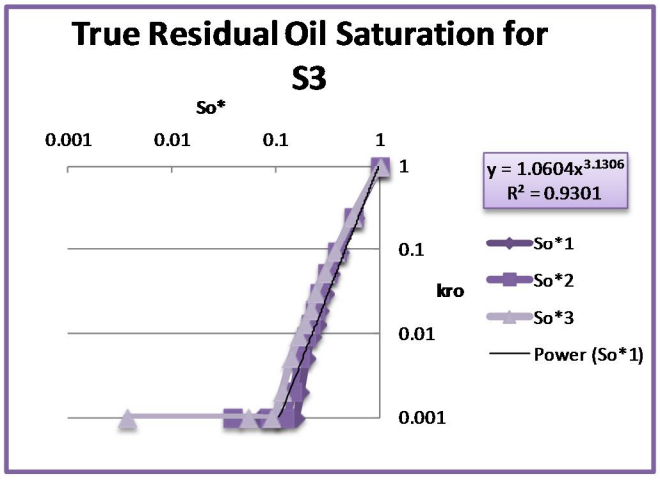

Fig (4-19): logarithmic scale of Kro Vs. So* for 3

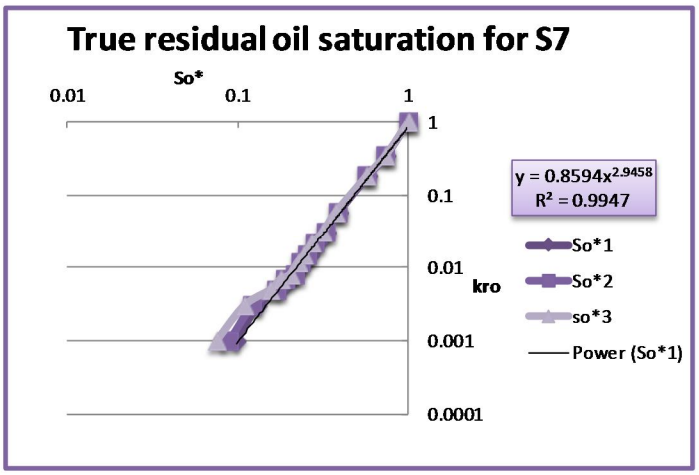

Fig (4-20): logarithmic scale Kro Vs. So* for 7

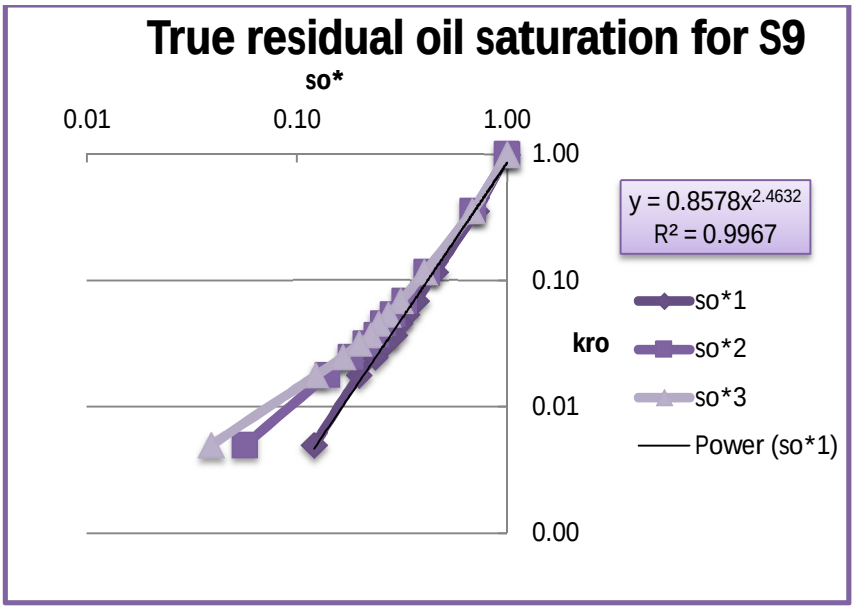

Fig (4-21): logarithmic scale Kro Vs. So* for 9

4.3.3 Estimating the K_{rw} End-Point:

This is an estimation of K_{rw} at true S_{or}. Plotting on log-log scale K_{rw} versus normalized water saturation (Sw*), Sw* was achieved using the following equation:

$$Sw* = \frac{Sw - Swi}{1 - Swi - Sor} \quad \text{..... (4.2)}$$

Where:

Sw* = Normalized water saturation

Sw = Water saturation

Swi = Initial water saturation

Sor = Critical oil saturation

Results of Sw* are shown in Tables below

For well 7:

Sample 3S

sw	Krw	sw*
0.443	-	0.000
0.503	0.029	0.233
0.535	0.04	0.358
0.557	0.05	0.444
0.577	0.061	0.521
0.597	0.07	0.599
0.615	0.083	0.669
0.631	0.096	0.732
0.644	0.107	0.782
0.656	0.119	0.829
0.676	0.14	0.907

Table (4-15): Sw* for Sample 3S

Sample 10S

sw	Krw	sw*
0.316	-	0.000
0.474	0.019	0.326
0.51	0.03	0.401
0.546	0.043	0.475
0.576	0.056	0.537
0.603	0.069	0.593
0.628	0.083	0.645
0.65	0.099	0.690
0.668	0.112	0.727
0.686	0.128	0.764
0.703	0.135	0.800
0.716	0.146	0.826
0.74	0.168	0.876
0.756	0.183	0.909
0.767	0.188	0.932

Table (4-16): Sw* for Sample 10S

SAMPLE 19S

SAMPLE 29S

sw	Krw	sw*
0.354	-	0.000
0.485	0.010	0.331
0.552	0.020	0.500
0.627	0.042	0.689
0.649	0.049	0.745
0.665	0.055	0.785
0.684	0.061	0.833
0.696	0.065	0.864
0.706	0.069	0.889
0.713	0.071	0.907
0.724	0.076	0.934
0.734	0.078	0.960

Table (4-17): Sw* for Sample 19S

sw	Krw	sw*
0.295	-	0.000
0.470	0.034	0.430
0.519	0.056	0.552
0.558	0.076	0.649
0.597	0.098	0.746
0.637	0.125	0.843
0.656	0.140	0.891
0.676	0.152	0.940
0.683	0.159	0.957
0.693	0.170	0.983

Table (4-18): Sw* for Sample 29S

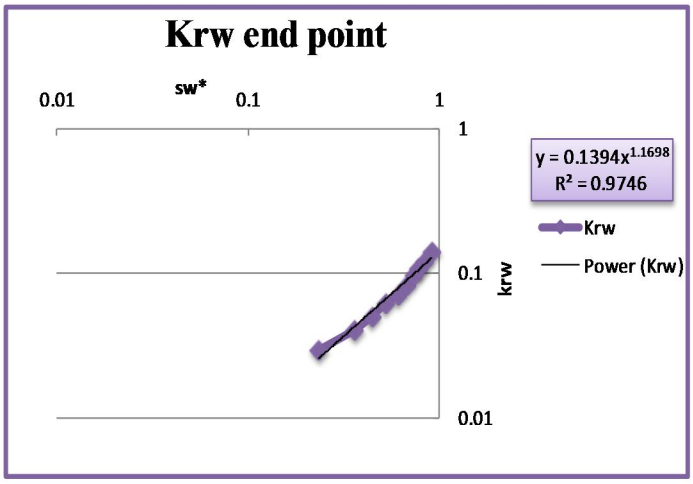

Fig (4-22): K_{rw} end point for 3S

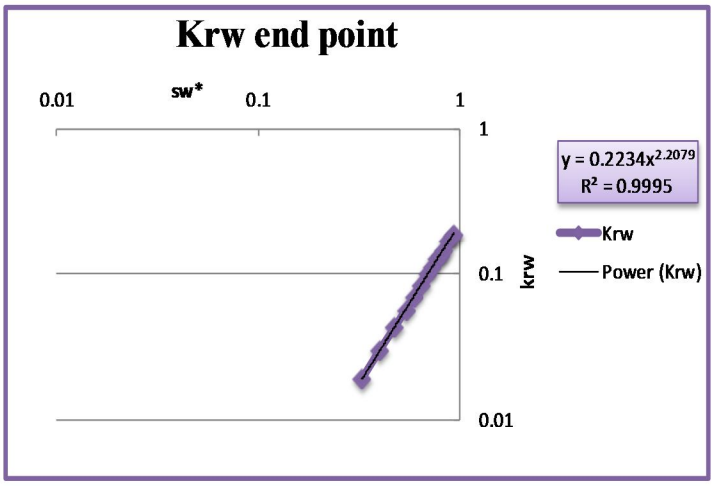

Fig (4-23): K_{rw} end point for 10S

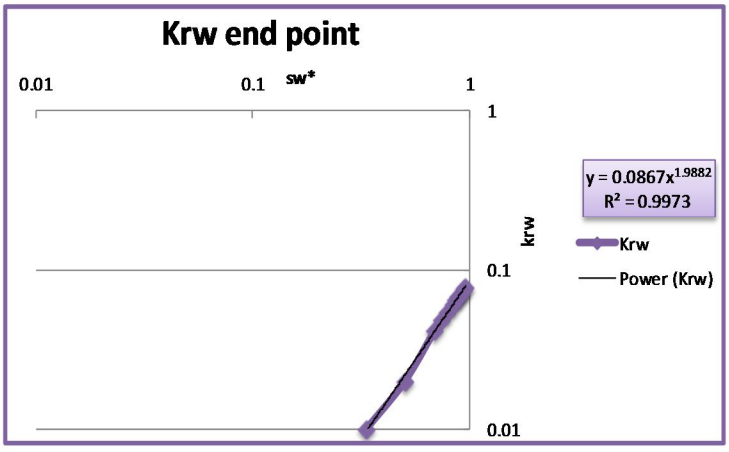

Fig (4-24): K_{rw} end point for 19S

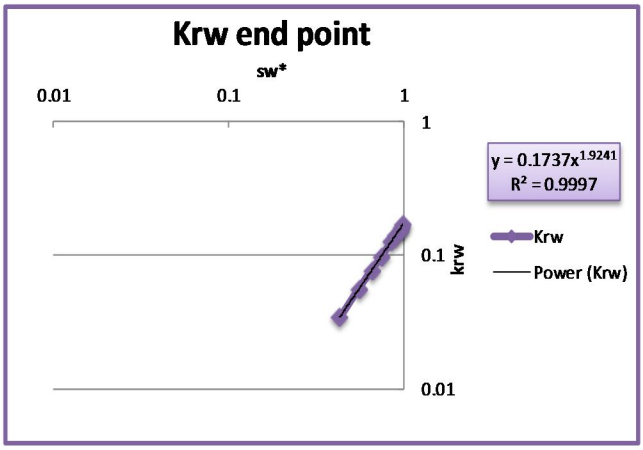

Fig (4-25): K_{rw} end point for 29S

For well 17:

Sample 3

sw	krw	Sw*
0.427	-	0.000
0.552	0.018	0.427
0.599	0.028	0.587
0.620	0.033	0.659
0.634	0.035	0.707
0.641	0.038	0.731
0.648	0.040	0.754
0.655	0.041	0.778
0.662	0.044	0.802
0.669	0.047	0.826
0.675	0.048	0.847
0.685	0.052	0.881
0.699	0.057	0.928
0.710	0.061	0.966

Table (4-19): Sw* for Sample 3

Sample 7

sw	krw	sw*
0.403	-	0.000
0.506	0.018	0.260
0.570	0.030	0.421
0.645	0.039	0.610
0.668	0.040	0.668
0.684	0.040	0.708
0.695	0.041	0.736
0.703	0.042	0.756
0.712	0.042	0.779
0.721	0.042	0.801
0.730	0.043	0.824
0.748	0.044	0.869
0.761	0.043	0.902
0.779	0.046	0.947
0.796	0.047	0.989

Table (4-20): Sw* for Sample 7

Sample 9

sw	krw	sw*
0.33	-	0.00
0.46	0.02	0.29
0.59	0.04	0.55
0.63	0.05	0.63
0.64	0.05	0.67
0.65	0.06	0.69
0.66	0.06	0.71
0.67	0.06	0.73
0.69	0.07	0.76
0.71	0.07	0.80
0.74	0.08	0.88
0.77	0.09	0.93

Table (4-21): Sw^* for sample 9

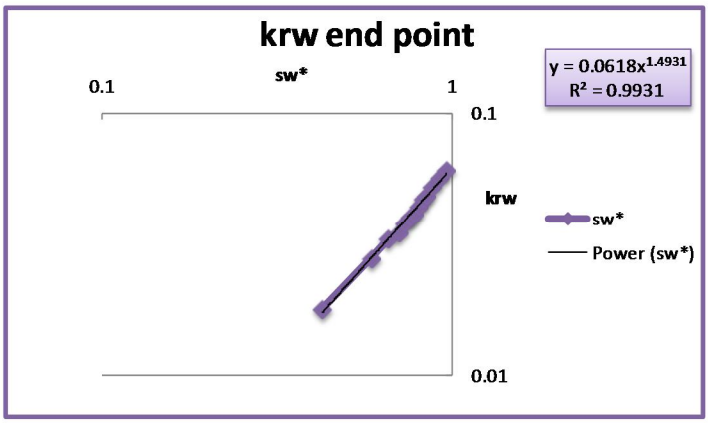

Fig (4-26): K_{rw} end point for S3

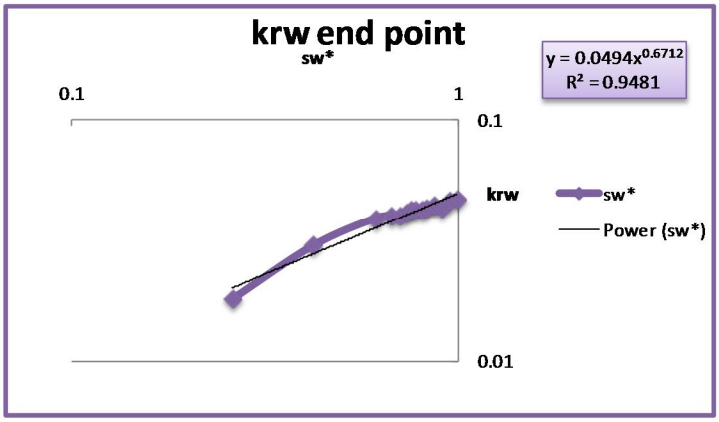

Fig (4-27): K_{rw} end point for S7

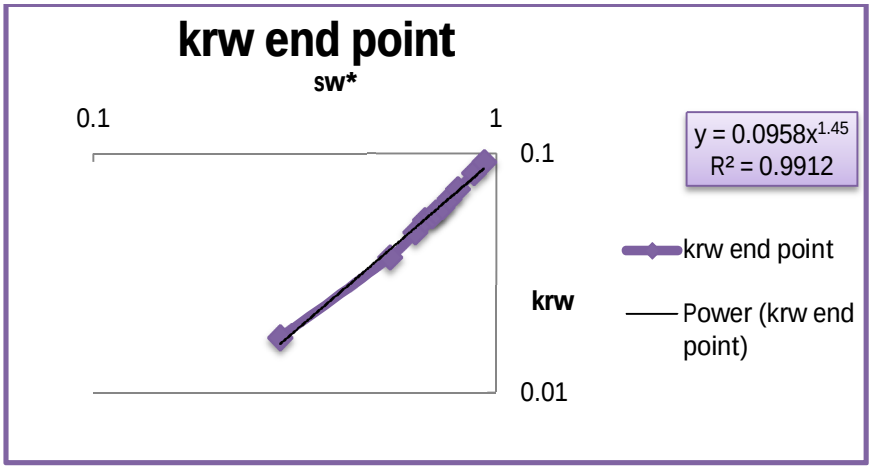

Fig (4-28): K_{rw} end point for S9

4.3.4 Calculating Refined Relative Permeability:

Refined relative permeability was calculated using the following equations:

$$\text{R-Kro} = (So*)^{No} \qquad \text{..... (4.3)}$$

$$\text{R-Krw} = (\text{Krw}^{*})\ (Sw*)^{Nw} \qquad \text{..... (4.4)}$$

Where:

R-Kro = refined relative permeability to oil

R-Krw = refined relative permeability to water

NO= Corey's Exponents for Oil

Nw= Corey's Exponents for water

Tables below show the calculation results which were plotted in figures

For well 7:

From figures (4-12 to 4-21) N_o is the slope of the true Sor straight line and N_w is the slope of krw end point line the values of N_o and N_w as follows:

Samples	N_o	N_w	K_{rw} end point
3S	2.9605	1.1698	0.1394
10S	2.1305	2.2079	0.2234
19S	2.2187	1.9882	0.0867
29S	1.4081	1.9241	0.1737

Sample 3S

	Lab data				Refine Peremability	
sw	kro	krw	sw*	so*	R-kro	R-krw

0.443	1.000	-	0.000	1.000	1.000	0.000
0.503	0.212	0.029	0.233	0.767	0.455	0.025
0.535	0.100	0.040	0.358	0.642	0.269	0.042
0.557	0.066	0.050	0.444	0.556	0.176	0.054
0.577	0.040	0.061	0.521	0.479	0.113	0.065
0.597	0.026	0.070	0.599	0.401	0.067	0.077
0.615	0.016	0.083	0.669	0.331	0.038	0.087
0.631	0.009	0.096	0.732	0.268	0.020	0.097
0.644	0.006	0.107	0.782	0.218	0.011	0.105
0.656	0.004	0.119	0.829	0.171	0.005	0.112
0.676	-	0.140	0.907	-		0.124

Table (4-22): Refined Relative Permeability for 3S

Sample 10S

	Lab data				Refine permeability	
sw	**kro**	**Krw**	**so***	**sw***	**R-kro**	**R-krw**
0.316	1.000	-	1.000	0.000	1.000	0.000
0.474	0.405	0.019	0.674	0.326	0.431	0.019
0.510	0.310	0.030	0.599	0.401	0.336	0.030
0.546	0.234	0.043	0.525	0.475	0.253	0.043
0.576	0.183	0.056	0.463	0.537	0.194	0.057
0.603	0.151	0.069	0.407	0.593	0.147	0.070
0.628	0.118	0.083	0.355	0.645	0.110	0.085
0.650	0.094	0.099	0.310	0.690	0.082	0.098
0.668	0.073	0.112	0.273	0.727	0.063	0.111
0.686	0.058	0.128	0.236	0.764	0.046	0.123
0.703	0.040	0.135	0.200	0.800	0.033	0.136
0.716	0.026	0.146	0.174	0.826	0.024	0.147
0.740	0.010	0.168	0.124	0.876	0.012	0.167
0.756	0.005	0.183	0.091	0.909	0.006	0.181
0.767	-	0.188	0.068	0.932	0.003	0.191

Table (4-23): Refined Relative Permeability for 10S

Sample 19S

	Lab data				Refine permeability	
sw	Kro	Krw	sw*	so*	R-kro	R-krw
0.354	1.000	-	0.000	1.000	1.000	0.000
0.485	0.270	0.010	0.331	0.669	0.410	0.010
0.552	0.120	0.020	0.500	0.500	0.215	0.022
0.627	0.043	0.042	0.689	0.311	0.075	0.041
0.649	0.028	0.049	0.745	0.255	0.048	0.048
0.665	0.020	0.055	0.785	0.215	0.033	0.054
0.684	0.012	0.061	0.833	0.167	0.019	0.060
0.696	0.008	0.065	0.864	0.136	0.012	0.065
0.706	0.005	0.069	0.889	0.111	0.008	0.069
0.713	0.004	0.071	0.907	0.093	0.005	0.071
0.724	0.002	0.076	0.934	0.066	0.002	0.076
0.734	-	0.078	0.960	0.040	0.001	0.080

Table (4-24): Refined Relative Permeability for 19S

Sample 29S

	Lab data				Refine permeability	
sw	kro	Krw	sw*	so*	R-kro	R-krw
0.295	1.000	-	0.000	1.000	1.000	0.000
0.470	0.316	0.034	0.430	0.570	0.453	0.034
0.519	0.210	0.056	0.552	0.448	0.323	0.055
0.558	0.147	0.076	0.649	0.351	0.229	0.076
0.597	0.090	0.098	0.746	0.254	0.145	0.099
0.637	0.049	0.125	0.843	0.157	0.074	0.125
0.656	0.031	0.140	0.891	0.109	0.044	0.139
0.676	0.015	0.152	0.940	0.060	0.019	0.154
0.683	0.010	0.159	0.957	0.043	0.012	0.160
0.693	-	0.170	0.983	0.017	0.003	0.168

Table (4-25): Refined Relative Permeability for 29S

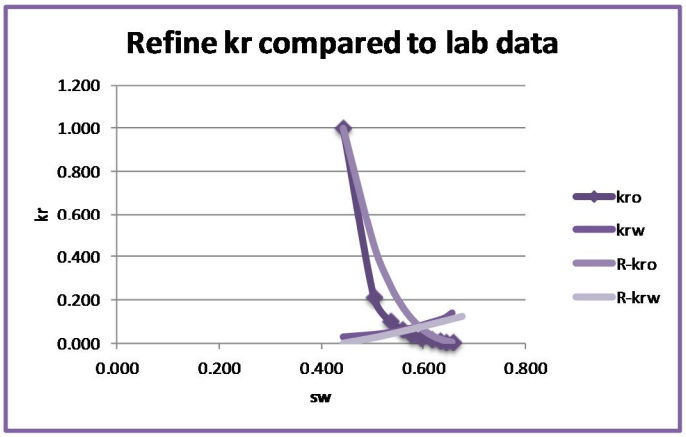

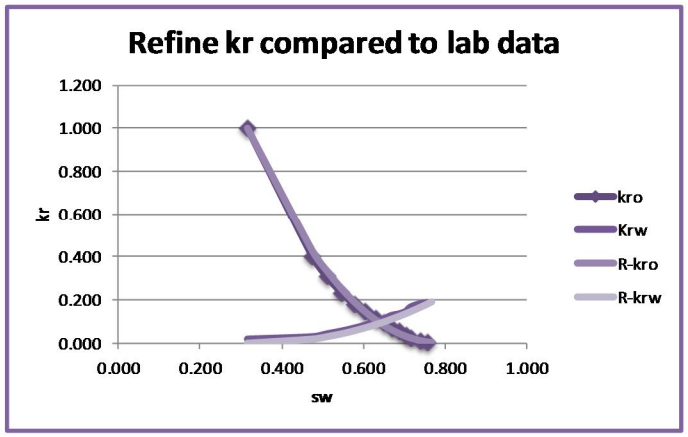

Fig (4-29): Refined curves for sample 3S

Fig (4-30): Refined Curves for sample 10S

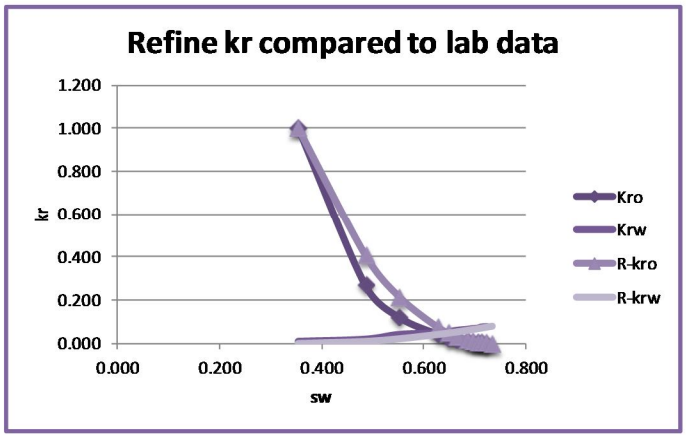

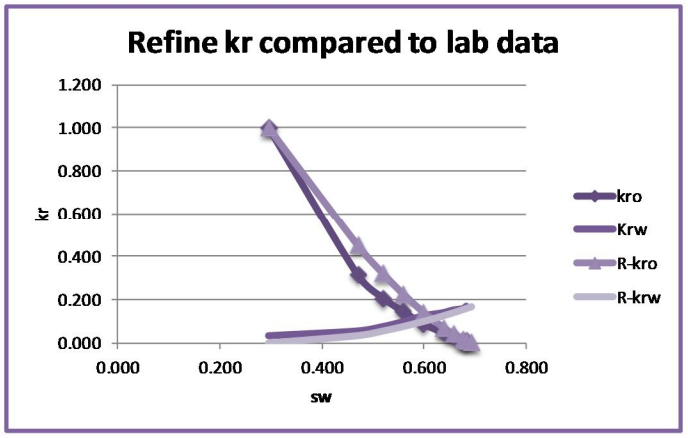

Fig (4-31): Refined curves for sample 19S

Fig (4-32): Refined Curves for sample 29S

For well 17:

Sample 3

	LabData				Refine Permeability	
Sw	**kro**	**krw**	**so***	**sw***	**R-kro**	**R-krw**
0.427	1.000	-	1.000	0.000	1.000	0.000
0.552	0.247	0.018	0.573	0.427	0.184	0.019
0.599	0.092	0.028	0.413	0.587	0.068	0.029
0.620	0.052	0.033	0.341	0.659	0.038	0.035
0.634	0.030	0.035	0.293	0.707	0.024	0.038
0.641	0.019	0.038	0.269	0.731	0.019	0.040
0.648	0.013	0.040	0.246	0.754	0.014	0.042
0.655	0.009	0.041	0.222	0.778	0.010	0.044
0.662	0.005	0.044	0.198	0.802	0.007	0.045
0.669	0.002	0.047	0.174	0.826	0.005	0.047
0.675	0.001	0.048	0.153	0.847	0.003	0.049
0.685	0.001	0.052	0.119	0.881	0.002	0.052
0.699	0.001	0.057	0.072	0.928	0.000	0.056
0.710	-	0.061	0.034	0.966	0.000	0.059

Table (4-26): Refined Relative Permeability for sample 3

Sample 7:

	Lab Data				Refine Permeability	
sw	**kro**	**krw**	**sw***	**So***	**R-kro**	**R-krw**
0.403	1.000	-	0.000	1.000	1.000	0.000
0.506	0.347	0.018	0.260	0.740	0.392	0.016
0.570	0.182	0.030	0.421	0.579	0.182	0.024
0.645	0.058	0.039	0.610	0.390	0.053	0.033
0.668	0.031	0.040	0.668	0.332	0.032	0.035
0.684	0.022	0.040	0.708	0.292	0.022	0.037
0.695	0.015	0.041	0.736	0.264	0.016	0.038
0.703	0.012	0.042	0.756	0.244	0.012	0.039
0.712	0.008	0.042	0.779	0.221	0.009	0.040
0.721	0.007	0.042	0.801	0.199	0.007	0.041
0.730	0.005	0.043	0.824	0.176	0.004	0.042
0.748	0.003	0.044	0.869	0.131	0.002	0.044
0.761	0.001	0.043	0.902	0.098	0.001	0.045
0.779	0.000	0.046	0.947	0.053	0.000	0.047
0.796	-	0.047	0.989	0.011	0.000	0.049

Table (4-27): Refined Relative Permeability for sample 7

Sample 9:

					Refine Permeability	
sw	**sw***	**So***	**kro**	**krw**	**R-kro**	**R-krw**
0.326	0.000	1.000	1.000	-	1.000	0.000
0.464	0.311	0.709	0.356	0.017	0.402	0.018
0.585	0.583	0.454	0.116	0.037	0.123	0.045
0.625	0.673	0.369	0.069	0.047	0.071	0.055
0.642	0.712	0.333	0.054	0.053	0.054	0.059
0.654	0.739	0.308	0.046	0.055	0.044	0.062
0.662	0.757	0.291	0.037	0.057	0.038	0.065
0.674	0.784	0.266	0.032	0.060	0.030	0.068
0.688	0.815	0.236	0.025	0.065	0.022	0.072
0.706	0.856	0.198	0.018	0.071	0.014	0.077
0.743	0.939	0.120	0.005	0.083	0.004	0.088
0.768	0.995	0.068	-	0.092	0.001	0.095

Table (4-28): Refined Relative Permeability for sample9

Fig (4-33): Refined curves for sample 3

Fig (4-34): Refined Curves for sample7

Fig (4-35): Refined Curves for sample9

4.3.5 Normalizing and De-Normalizing Samples:

To get smooth curves normalized and de-normalized values were calculated as in tables below and plotted in figures using the following equations:

$$Sw* = \frac{Sw - Swc}{1 - Swc - Sor} \quad \text{……..} \quad (4.5)$$

$$Kro* = \frac{Kro}{Kro*(@swi)} \quad \text{……} \quad (4.6)$$

$$Krw* = \frac{Krw}{Krw*(@sor)} \quad \text{……} \quad (4.7)$$

Where

Sw*= normalized water saturation

Kro*= normalized oil relative permeability

Krw*= normalized water relative permeability

Kro*(@swi) = oil relative permeability at the initial water saturation

Krw*(@sor) = water relative permeability at the residual oil saturation

For well 7:

Sample 3S

Sw	R-kro	R-krw	Sw*	kro*	krw*
0.443	1.000	0.000	0.000	1.000	0.000
0.503	0.455	0.025	0.233	0.455	0.182
0.535	0.269	0.042	0.358	0.269	0.301
0.557	0.176	0.054	0.444	0.176	0.386
0.577	0.113	0.065	0.521	0.113	0.467
0.597	0.067	0.077	0.599	0.067	0.549
0.615	0.038	0.087	0.669	0.038	0.625
0.631	0.020	0.097	0.732	0.020	0.694
0.644	0.011	0.105	0.782	0.011	0.750
0.656	0.005	0.112	0.829	0.005	0.803
0.676	0.000	0.124	0.907	0.000	0.892

Table (4-29): Normalized values (3S)

Sample 10S

Sw	R-kro	R-krw	Sw*	kro*	krw*
0.316	1.000	0.000	0.000	1.000	0.000
0.474	0.431	0.019	0.326	0.431	0.084
0.510	0.336	0.030	0.401	0.336	0.133
0.546	0.253	0.043	0.475	0.253	0.193
0.576	0.194	0.057	0.537	0.194	0.254
0.603	0.147	0.070	0.593	0.147	0.315
0.628	0.110	0.085	0.645	0.110	0.379
0.650	0.082	0.098	0.690	0.082	0.441
0.668	0.063	0.111	0.727	0.063	0.495
0.686	0.046	0.123	0.764	0.046	0.553
0.703	0.033	0.136	0.800	0.033	0.610
0.716	0.024	0.147	0.826	0.024	0.656
0.740	0.012	0.167	0.876	0.012	0.747
0.756	0.006	0.181	0.909	0.006	0.810
0.767	0.003	0.191	0.932	0.000	0.856

Table (4-30): Normalized values (10S)

Sample 19S

Sw	R-kro	R-krw	Sw*	kro*	krw*
0.354	1.000	0.000	0.000	1.000	0.000
0.485	0.410	0.010	0.331	0.410	0.111
0.552	0.215	0.022	0.500	0.215	0.252
0.627	0.075	0.041	0.689	0.075	0.477
0.649	0.048	0.048	0.745	0.048	0.557
0.665	0.033	0.054	0.785	0.033	0.619
0.684	0.019	0.060	0.833	0.019	0.696
0.696	0.012	0.065	0.864	0.012	0.747
0.706	0.008	0.069	0.889	0.008	0.791
0.713	0.005	0.071	0.907	0.005	0.823
0.724	0.002	0.076	0.934	0.002	0.874
0.734	0.001	0.080	0.960	0.000	0.921

Table (4-31): Normalized values (19S)

Sample 29S

Sw	R-kro	R-krw	Sw*	kro*	krw*
0.295	1.000	0.000	0.000	1.000	0.000
0.470	0.453	0.034	0.430	0.453	0.197
0.519	0.323	0.055	0.552	0.323	0.318
0.558	0.229	0.076	0.649	0.229	0.435
0.597	0.145	0.099	0.746	0.145	0.569
0.637	0.074	0.125	0.843	0.074	0.720
0.656	0.044	0.139	0.891	0.044	0.802
0.676	0.019	0.154	0.940	0.019	0.888
0.683	0.012	0.160	0.957	0.012	0.918
0.693	0.003	0.168	0.983	0.000	0.967

Table (4-32): Normalized values (29S)

Fig (4-36): Normalized Curve (3S)

Fig (4-37): Normalized Cure (10S)

Fig (4-38): Normalized Curve (19S)

Fig (4-39): Normalized Cure (29S)

For well 17

Sample 3

Sw	R-kro	R-krw	sw*	kro*	krw*
0.427	1.000	0.000	0.000	1.000	0.000
0.552	0.184	0.019	0.427	0.184	0.309
0.599	0.068	0.029	0.587	0.068	0.482
0.620	0.038	0.035	0.659	0.038	0.566
0.634	0.024	0.038	0.707	0.024	0.624
0.641	0.019	0.040	0.731	0.019	0.654

0.648	0.014	0.042	0.754	0.014	0.684
0.655	0.010	0.044	0.778	0.010	0.714
0.662	0.007	0.045	0.802	0.007	0.745
0.669	0.005	0.047	0.826	0.005	0.776
0.675	0.003	0.049	0.847	0.003	0.803
0.685	0.002	0.052	0.881	0.002	0.849
0.699	0.000	0.056	0.928	0.000	0.913
0.710	0.000	0.059	0.966	0.000	0.965

Table (4-33): Normalized values (sample3)

Sample 7

sw	R-kro	R-krw	sw*	kro*	krw*
0.403	1.000	0.000	0.000	1.000	0.000
0.506	0.392	0.016	0.260	0.392	0.346
0.570	0.182	0.024	0.421	0.182	0.515
0.645	0.053	0.033	0.610	0.053	0.699
0.668	0.032	0.035	0.668	0.032	0.753
0.684	0.022	0.037	0.708	0.022	0.790
0.695	0.016	0.038	0.736	0.016	0.816
0.703	0.012	0.039	0.756	0.012	0.834
0.712	0.009	0.040	0.779	0.009	0.855
0.721	0.007	0.041	0.801	0.007	0.875
0.730	0.004	0.042	0.824	0.004	0.896
0.748	0.002	0.044	0.869	0.002	0.936
0.761	0.001	0.045	0.902	0.001	0.965
0.779	0.000	0.047	0.947	0.000	1.000
0.796	0.000	0.049	0.989	0.000	

Table (4-34): Normalized values (sample7)

Sample 9

sw	R-kro	R-krw	sw*	kro*	krw*
0.326	1.000	0.000	0.000	1.000	0.000
0.464	0.402	0.018	0.311	0.402	0.199
0.585	0.123	0.045	0.583	0.123	0.486
0.625	0.071	0.055	0.673	0.071	0.595
0.642	0.054	0.059	0.712	0.054	0.644
0.654	0.044	0.062	0.739	0.044	0.679
0.662	0.038	0.065	0.757	0.038	0.702
0.674	0.030	0.068	0.784	0.030	0.738
0.688	0.022	0.072	0.815	0.022	0.780
0.706	0.014	0.077	0.856	0.014	0.836
0.743	0.004	0.088	0.939	0.004	0.953
0.768	0.001	0.095	0.995	0.000	1.000

Table (4-35): Normalized values (sample9)

Fig (4-40): Normalized Curve (sample3)

Fig (4-41): Normalized Cure (Sample7)

Fig (4-42): Normalized Cure (Sample9)

4.3.6 Averaging Normalized Data:

To get one system from all samples, averages normalized and choose arbitrary values of Sw*and calculate the cross values of kro and krw then use calculations as following:

$$\mathbf{Kro * a} = \frac{\mathbf{SUM\ (h*k*kro*)}}{\mathbf{SUM\ (h*k)}} \qquad \text{..... (4.8)}$$

$$\mathbf{Krw * a} = \frac{\mathbf{SUM\ (h*k*krw*)}}{\mathbf{SUM\ (h*k)}} \qquad \text{..... (4.9)}$$

Where

H= the thickness

K= the absoulate permeability

For well 7:

Table (4-36): Average Normalized values for well 7

Fig (4-43): Average Normalized Curve for well 7

For well 17

Table (4-37): Average Normalized values for well 17

Fig (4-44): Average Normalized Curve for well 17

4.3.7 De-Normalizing Average Data:

The de-normalization data were calculated to represent the final relative permeability system for Bentiu formation. Using the following equations:

$$\mathbf{Kro} = (\mathbf{Kro}*)\mathbf{avg} * (\mathbf{Kro})\mathbf{swi} \quad \ldots\ldots\ldots\ldots\ldots\ldots \textbf{(4.10)}$$

$$\mathbf{Krw} = (\mathbf{Krw}*)\mathbf{avg} * (\mathbf{Krw})\mathbf{sor} \quad \ldots\ldots\ldots\ldots\ldots \textbf{(4.11)}$$

$$\mathbf{Sw = (Sw*)avg * (1 - Swi - Sor) + Swi \quad \ldots\ldots\ldots\ldots \quad (4.12)}$$

$$\mathbf{(Kro)Swi = SUM\ (h * k * (kro)swi)/(SUM(h * k))} \quad \ldots\ldots \quad \mathbf{(4.13)}$$

$$\mathbf{(Krw)Sor = SUM\ (h * k * (krw)sor)/(SUM(h * k))} \quad \ldots\ldots\ldots \quad \mathbf{(4.14)}$$

Where:

Swi = initial water saturation

Sor = residual oil saturation

Kro(swi) = oil relative permeability at the initial water saturation

Krw(sor) = water relative permeability at the residual oil saturation

H = thickness

K = absolute permeability

For well 7

Table (4-38): De-normalization data for well 7

Fig (4-45): the final Relative Permeability Curve for well 7

From relative permeability curve above, the values of initial water saturation (S_{wi}) and residual oil saturation (S_{or}), are **0.352** and **0.263** respectively. While the K_{ro} at S_{wi} is **1** and K_{rw} at S_{or} is **0.156**.

For well 17

Table (4-39): De-normalization data for well 17

Fig (4-46): the final Relative Permeability Curve for well 17

From relative permeability curve above, the values of initial water saturation (S_{wi}) and residual oil saturation (S_{or}), are **0.385** and **0.227** respectively. While the K_{ro} at S_{wi} is **1** and K_{rw} at S_{or} is **0.082**.

The determination of wettability of a sample from permeability data is accomplished by observing the intersection of the final relative permeability curve and the value of water permeability at residual oil saturation if the intersection is greater than 0.5 and the value of water permeability at residual oil saturation (Krw(sor)) is less than 0.3 then the sample is considered to be water-wet, and if the intersection is less than 0.5 and Krw(sor) is greater than 0.3 then the sample is considered oil- wet.

According to this conditions well 7 (intersection at 0.61 and Krw at sor = 0.156) and well 17 (intersection at 0.65 and Krw at sor = 0.082) systems consider strong water- wet.

4.4 Capillary Pressure Analysis:

Capillary pressure laboratory data for seven samples from well 7 and well 17 were available for this study. Tables below show these data.

For well 7

Oil-Brine Capillary Pressure by the Centrifuge Technique data

Table (4-40) Pc Lab Data for S3 **Table (4-41) Pc Lab Data for S18** **Table (4-42) Pc Lab Data for S53**

Table (4-43) Pc Lab Data for S85

4.4.1 Plot Laboratory Data:

We first plot the capillary pressure measured at laboratory conditions versus water saturation for the four samples as shown in figures below

Fig (4-47): P_c (lab) Vs. S_w for S3

Fig (4-48): P_c (lab) Vs. S_w for S18

Fig (4-49): P_c (lab) Vs. S_w for S53

Fig (4-50): P_c (lab) Vs. S_w for S85

For well 17

Air-Brine Capillary Pressure by Porous Plate Method at room condition data

Table (4-44) Pc Lab Data for S4 **Table (4-45) Pc Lab Data for S8** **Table (4-46) Pc Lab Data for S10**

Fig (4-51): P_c (lab) Vs. S_w for S4 **Fig (4-52): P_c (lab) Vs. S_w for S8**

Fig (4-53): P_c (lab) Vs. S_w for S10

4.4.2 Converting Capillary Pressure Data:

At this step the capillary pressure data obtained from laboratory at laboratory conditions are converted to capillary pressure at reservoir conditions using the following equation:

$$\mathbf{Pcres = Pclab \frac{\sigma 2 \cos\theta 2}{\sigma 1 \cos\theta 1}} \quad \text{..... (4.15)}$$

Where

pc_{res} = oil-brine capillary pressure (reservoir), psia

Pc_{lab} = air-brine capillary pressure, psia

σ_2 = interfacial tension between oil and brine (reservoir) (30)

Θ_2 = contact angle between oil and brine (reservoir) (30)

σ_1 = interfacial tension between air and brine

Θ_1 = contact angle between air and brine

For well 7

$\sigma_{res} \cos(\theta_{res}) = 26$

$\sigma_{lab} \cos(\Theta_{lab}) = 72$

Table (4-47): P_c (Res.) for sample 3

Table (4-48): P_c (Res.) for sample 18

Table (4-49): P_c (Res.) for sample53

Table (4-50): P_c (Res.) for sample 85

Fig (4-54): P_c (res) for S3

Fig (4-55): P_c (res) for S18

Fig (4-56): P_c (res) for S53

Fig (4-57): P_c (res) for S85

For well 17

Table (4-51): P_c (Res.) for sample 4

Table (4-52): P_c (Res.) for sample 8

Table (4-53): P_c (Res.) for sample 10

Fig (4-58): P_c (res) for S4

Fig (4-59): P_c (res) vs. S_w for S8

Fig (4-60): P_c (res) for S8

4.4.3 Calculate J function:

Capillary pressure data obtained from core samples represents only a small part of the reservoir. Therefore it is necessary to averaging all the capillary data to classify a particular reservoir. The average values were calculated using the following equation

$$J = \frac{0.2166 \cdot Pc \cdot \sqrt{(\frac{K}{\emptyset})}}{\sigma \cdot \cos\theta} \quad \text{..... (4.16)}$$

Where:

J = Leverett capillary pressure function, dimensionless

Pc= Capillary pressure, psia

σ = Air-brine interfacial tension

Θ = Air-brine contact angle

K = permeability

φ = porosity

For well 7

Table (4-54): J function for Sample 3

Table (4-55): J function for Sample18

Table (4-56): J function for Sample 53

Table (4-57): J function for Sample 85

Fig (4-61): J function (S3)

Fig (4-62): J function (S18)

Fig (4-63): J function (S53)

Fig (4-64): J function (S85)

For well 17

Table (4-58): J function for Sample 4

Table (4-59): J function for Sample 8

Table (4-60): J function for Sample 10

Fig (4-65): J function (S4)

Fig (4-66): J function (S8)

Fig (4-67): J function (S10)

4.4.4 Grouping samples:

Plot J-Function VS Sw for all samples and determines best fit correlation for the group

Then use the J function equation from the trend line to calculate the Pc reservoir of the group

For well 7

Table (4-61) grouping samples of well 7 **Fig (4-68) grouping samples of well 7 and determine the best fit**

For well 17

Table (4-62) grouping samples of well 17

Fig (4-69) grouping samples of well 17 and determine the best fit

4.4.5 Calculate the reservoir pressure (Pc_{res}) for the group:

From step 4.4.4 figures use the trend line equation to calculate (**Pc_{res}**) as following

For well 7

From figure (4-68) J function equation as following

$J = 0.1079*S_w^{(-4.591)}$

Average values:

Table (4-63) reservoir pressure of well 7 **Fig (4-70) reservoir pressure of well 7**

For well 17

From figure (4-69) J function equation as following

$J = 0.0267 * S_w^{\wedge(-6.716)}$

Average values:

Table (4-64) reservoir pressure of well 17

Fig (4-71) reservoir pressure of well 17

4.4.6 Convert reservoir pressure to height:

Calculate the height and then plot it VS Water saturation to estimate the transition zone height and use the trend line equation to generate water saturation logging track. Height equation as following

$$H = \frac{144\ Pc}{\rho w - \rho o} \quad \text{..... (4.17)}$$

Where

H = height

Pc = reservoir pressure

ρ_w = water density

ρ_o =oil density

For well 7

Water density = 65.2

Oil density = 55.2

Sw	Pcres	H,ft	H,m
1.000	0.222	3.199	0.975
0.950	0.281	4.048	1.234
0.900	0.360	5.189	1.581
0.850	0.468	6.745	2.056
0.800	0.619	8.910	2.716
0.750	0.832	11.983	3.652
0.700	1.142	16.449	5.014
0.650	1.605	23.115	7.045
0.600	2.318	33.379	10.174
0.550	3.456	49.770	15.170
0.500	5.354	77.090	23.497
0.450	8.684	125.047	38.114
0.400	14.913	214.741	65.453
0.350	27.529	396.420	120.829
0.300	55.866	804.467	245.202
0.278	79.250	1141.202	347.838

Table (4-65): the height calculations for well 7

Fig (4-72): height of well 7

For well 17

Sw	Pcres	H,ft	H,m
1.000	0.287	4.132	1.259
0.950	0.405	5.831	1.777
0.900	0.582	8.384	2.555
0.850	0.855	12.307	3.751
0.800	1.284	18.492	5.636

0.750	1.981	28.524	8.694
0.700	3.148	45.337	13.819
0.650	5.179	74.576	22.731
0.600	8.865	127.663	38.912
0.550	15.903	229.008	69.802
0.500	30.164	434.355	132.391
0.414	107.150	1542.954	470.292

Table (4-66): the height calculations for well 17

Fig (4-73): height of well 17

From the capillary pressure curves that described above it is clear that the system is two phase and there is no sign of a single phase at all which means all the wells perforated at this formation will produce two phase (Oil + Water) from day 1.and from fig(4-72) we can estimate the transition zone height for well 7 is 140m, the saturation equation is ($0.975*x^{\wedge(-4.591)}$) and from fig (4-73) it's obvious that the transition zone height for well 17 is 190m and the saturation equation is($1.2593*x^{\wedge(-6.716)}$) .

4.5 Well logging:

4.5.1 Wireline logging interpretation using interactive petrophysics software:

Interactive PetrophysicsTM (IP) was developed by a Petrophysicist, with a view to work as petrophysicists want to work, but never thought possible! The software is different by design - portable, quick and versatile. It is an easy to use log analysis tool, ideal for both geoscientists and petrophysicists. Geoscientists may wish to quality check of their log data and experienced Petrophysicists can carry out multi-zone, multi-well petrophysical field analyses. Interactive Petrophysics has been developed over 12 years and is now used by over 300 companies, in more than 70 countries globally. The heart of IP is its graphical interpretation engine. This allows the user to perform a fast and sophisticated multi-zone interpretation using only the mouse, adjusting parameters on log plots, crossplots and histograms. The data from three wells (well 3, well 7 and well 17) entered to IP software to identify the lithology and hydrocarbon zones and calculate the porosity and water saturation using interpretation menu in the toolbar.

The conventional well log interpretation usually contains three tracks of log sets to determine the different petrophysics properties, the well log data displayed in basic three tracks as follow: The first track contains Caliper log (HCAL), bit size log (BS) and Gamma ray log (GR) to determine the lithologies and hardness of the formation. The second track contain resistivity logs which measure the resistivity in three zones which are: the resistivity of invaded zone (RXOZ), the resistivity of transmission zone (HLLS) and the resistivity of uninvaded zone (HLLD), and from which we can determine the true resistivity for the formation (RT) that can be used in saturation calculation and other parameter estimation. The last track contains porosity logs: the Neutron log (NPHI), density log (RHOZ) and Sonic log (DT) which measure the porosity through three different tools.

4.5.2 Lithology identification:

We can use Gamma ray tool to identify lithology (whether sand or shale) which measure the natural gamma ray emission from the formation. The shale emits relatively high amount of gamma ray naturally because the presence of potassium (K) and the sand emit relatively low amount of gamma ray. Hence, the higher gamma ray value form the formation means shale and lower value means sand. The gamma ray log (GR) displayed in the first track (from 0-150 GAR) to discriminate between sand and shale , and the gamma ray base line considered (60 GAR),

every value less than the base line considered sand and every value more than the base line considered shale. For example depth interval (1125to 1155 m) of Bentiu Formation from SA-1 considered shelly sand (fig. 4.74.).

The Caliper log (HCAL) displayed in the first track (from 6-16 inch) to determine the hardness of formation by measuring the borehole diameter, and the base line is the bit size (12.25 inch). In the sand formation if the log value and caliper log base line are coincided that means hard sand, and if the caliper log value is greater than base line that means friable sand. In case where the caliper logs value is less than the base line that indicate to mud cake forming in the permeable zones. In the shale formation usually the caliper log value is more than the base line as result of shale swelling which decrease the wellbore diameter. For example in (fig.4.74.) the sand zone (1125to 1155 m) considered hard sand because the caliper log and bit size are coincided.

Fig (4-74): gamma ray & caliper log in SA-1 between (1125to 1155 m)

4.5.3 Porosity logs:

The Neutron log, density log and sonic log are displayed in the third track to determine the porosity of the formation as follow: The Neutron log (NPHI) displayed in the third track (from .45 to - .15) which measures the porosity filled with fluid by measuring the amount of the hydrogen in formation fluids (water, oil and gas). Usually the Neutron log less accurate in the gas zones because the concentration of hydrogen in gas zones is less than water and oil formation result in low porosity value than the true porosity. Hence, the neutron log in gas zones compared with the other porosity logs.

Fig (4.75): neutron and density log in SA-1 between (1125to 1155m)

4.5.4 Resistivity logs:

The resistivity logs displayed in the third track in logarithmic scale (from 0.02 to 2000 OHMM), the lateral resistivity device measures the resistivity in three zones which are: The resistivity of invaded zone (RXOZ), the resistivity of transmission zone or shallow resistivity

(HLLS) and the resistivity of un invaded zone or deep resistivity (HLLD), and from which we can determine the true resistivity for the formation (RT) using charts ,equations or in this case directly by interactive petrophysics (IP) software.

Fig (4.76): resistivity logs in SA-1 between (1125to 1155m)

4.6 Calculations and results:

4.6.1: Shale volume from gamma ray log:

Using IP software shale volume can be calculated directly by Clicking on the interpretation tool bar and select the tab clay volume from the drop dawn list and then select the type of correction (GR correction) and the software will calculate the shale volume for the selected zones (target zones).

It is obvious that there are no sign of clean sand; all the target zones are shelly sand except well 7 has the lowest shale contents.

For well 3:

Well 3 has four shelly sand target zones

Zones	Top	Bottom	(Vsh)avg	Description
SA-1	1125	1155	0.371	the highest value
SA-2	1164.2	1165.9	0.233	the lowest value
SA-3	1174.4	1179	0.242	
SA-4	1181.6	1190.2	0.312	

Figure (4-77) and figure (4-78) display the calculated shale volume in well 3 for the target zones from SA-1 to SA-4

Fig (4-77): shale volume calculation in SA-1 between (1125to 1155m)

Fig (4-78): shale volume calculation in well 3 SA-2(1164.2to 1165.9m),

SA-3 (1174.4 to 1179), SA-4 (1181.6 to 1190.2)

For well 17:

In well 17 there are also four target zones

Zones	Top	Bottom	(Vsh)avg	Description
S-1	1409.1	1414	0.204	
S-2	1453.7	1456	0.165	The lowest value
S-3	1603.7	1606.7	0.214	The highest value
S-4	1676.5	1681.8	0.17	

Fig (4-79): shale volume calculation in well 17 S-1 and S-2

Fig (4-80): shale volume calculation in well 17 S-3 and S-24

For well 17:

Well 17 has eleven complicated target zones

Zones	Top	Bottom	(Vsh)avg	Description
SO-1	2031.9	2039.3	0.145	
SO-2	2045.8	2055.1	0.213	The highest value
SO-3	2151.3	2163.5	0.114	
SO-4	2167.4	2172.2	0.118	
SO-5	2174	2176.7	0.076	
SO-6	2185.9	2191.5	0.013	

SO-7	2218.2	2239.1	0.098	
SO-8	2249.3	2270	0.09	
SO-9	2276.9	2282.5	0.009	The lowest value
SO-10	2285.4	2300	0.083	
SO-11	2461.6	2467.7	0.081	

Fig (4-81): shale volume calculation in well 7 SO-1 and SO-2

Fig (4-82): shale volume calculation in well 7 SO-3, SO-4, SO-5 and SO-6

Fig (4-83): shale volume calculation in well 7 SO-7, SO-8, SO-9 and SO-10

4.6.2 Porosity and water saturation calculation:

To calculate porosity and saturation using IP software click on the interpretation tool bar and choose porosity and water saturation option to open multi choice window demands you to select all the necessary conditions like saturation equations and the desire method to calculate porosity (in this case use neutron density cross plots) the unites …. Etc. at the end click ok to show excessive plot contain (porosity, saturation, lithology, logic, gamma ray, resistivity… etc.)

For well 3

Fig (4-84): porosity and water saturation for well 3

For well 7:

Fig (4-85): porosity and water saturation for well 7 SO-1 and SO-2

Fig (4-86): porosity and water saturation for well 7 SO-3, SO-4, SO-5, and SO-6

Fig (4-87): porosity and water saturation for well 7 SO-7, SO-8, SO-9, and SO-10

For well 17:

Fig (4-88): porosity and water saturation for well 17 S-1 and S-2

Fig (4-89): porosity and water saturation for well 17 S-3 and S-4

4.6.3 Cuttoff calculations and results:

At the seam drop dawn list in the tool bar after porosity and water saturation there are the cutoff and summation option which include all the previous results of shale volume, porosity, gross, saturation for reservoir and pay zones

For well 3:

				Reservoir Summary						
Zone Name	**Top**	**Bottom**	**Gross**	**Net**	**N/G**	**Av phi**	**Av sw**	**Av Vcl Ari**	**Phi*H**	**PhiSo**
SA-1	1125	1155	30	9.3	0.31	0.159	0.37	0.371	1.48	0.93
SA-2	1164.2	1166.01	1.81	0.91	0.505	0.2	0.218	0.233	0.18	0.14
SA-3	1174.4	1179.73	5.33	4.57	0.858	0.217	0.26	0.242	0.99	0.73
SA-4	1185.67	1191.46	5.79	2.44	0.421	0.209	0.296	0.312	0.51	0.36
All zones	1125	1191.46	42.93	17.22	0.401	0.184	0.315	0.321	3.16	2.17

Table (4-67): Reservoir Cuttoff results for well 3

				Pay Summary						
Zone Name	**Top**	**Bottom**	**Gross**	**Net**	**N/G**	**Av phi**	**Av sw**	**Av Vcl Ari**	**Phi*H**	**PhiSo**
SA-1	1125	1155	30	8.69	0.29	0.159	0.36	0.367	1.38	0.8
SA-2	1164.2	1166.01	1.81	0.91	0.505	0.2	0.218	0.233	0.18	0.1
SA-3	1174.4	1179.73	5.33	4.57	0.858	0.217	0.26	0.242	0.99	0.7

SA-4	1185.67	1191.46	5.79	2.44	0.421	0.209	0.296	0.312	0.51	0.3
All zones	1125	1191.46	42.93	16.61	0.387	0.185	0.308	0.317	3.07	2.1

Table (4-68): Pay Cuttoff results for well 3

Observations:

Zone three (SA-3) from 1174.4 to 1179.73 m is the best zone since it has the highest porosity and lowest shale volume, reasonable thickness and good water saturation.

Fig (4-90): Cuttoff for well 3

For well 17:

				Reservoir Summary						
Zone Name	**Top**	**Bottom**	**Gross**	**Net**	**N/G**	**Av phi**	**Av Sw**	**Av Vcl Ari**	**Phi*H**	**PhiSo**
S-1	1409.1	1414	4.9	2.36	0.482	0.18	0.456	0.204	0.42	0.23
S-2	1453.7	1456	2.3	1.07	0.464	0.241	0.213	0.165	0.26	0.2
S-3	1603.7	1606.7	3	1.52	0.508	0.2	0.326	0.214	0.31	0.21
S-4	1676.5	1681.8	5.3	3.89	0.733	0.237	0.298	0.17	0.92	0.65
All zones	1409.1	1681.8	15.5	8.84	0.57	0.216	0.326	0.186	1.91	1.29

Table (4-69): Reservoir Cuttoff results for well 17

				Pay Summary						
Zone Name	**Top**	**Bottom**	**Gross**	**Net**	**N/G**	**Av phi**	**Av sw**	**Av Vcl Ari**	**Phi*H**	**PhiSo**
S-1	1409.1	1414	4.9	1.75	0.358	0.185	0.395	0.192	0.32	0.2
S-2	1453.7	1456	2.3	1.07	0.464	0.241	0.213	0.165	0.26	0.2
S-3	1603.7	1606.7	3	1.52	0.508	0.2	0.326	0.214	0.31	0.21
S-4	1676.5	1681.8	5.3	3.89	0.733	0.237	0.298	0.17	0.92	0.65
All zones	1409.1	1681.8	15.5	8.23	0.531	0.22	0.308	0.182	1.81	1.25

Table (4-70): Pay Cuttoff results for well 17

Fig (4-91): Cuttoff for well 17 S-1and S-2

Fig (4-92): Cuttoff for well 17 S-3 and S-4

For well 7:

Reservoir Summary										
Zone Name	**Top**	**Bottom**	**Gross**	**Net**	**N/G**	**Av phi**	**Av Sw**	**Av Vcl Ari**	**Phi*H**	**PhiSo***
SO-1	2031.9	2039.3	7.4	7.1	0.959	0.158	0.841	0.145	1.12	0.18
SO-2	2045.8	2051.46	5.66	1.68	0.296	0.148	0.525	0.213	0.25	0.12
SO-3	2151.3	2164.54	13.24	7.98	0.603	0.155	0.842	0.114	1.23	0.2
SO-4	2166.98	2172.2	5.22	4.57	0.875	0.154	0.836	0.118	0.7	0.12
SO-5	2174	2177.95	3.95	3.57	0.904	0.147	0.632	0.076	0.52	0.19
SO-7	2218.2	2239.1	20.9	18.61	0.891	0.15	0.766	0.098	2.8	0.65
SO-8	2248.81	2270	21.19	18.75	0.885	0.147	0.886	0.09	2.76	0.31
SO-9	2276.9	2282.5	5.6	3.54	0.632	0.141	0.784	0.009	0.5	0.11
SO-10	2285.4	2300.94	15.54	13.11	0.844	0.143	0.787	0.083	1.88	0.4
SO-11	2461.11	2467.7	6.59	5.18	0.786	0.14	0.927	0.081	0.72	0.05
All zones	2031.9	2467.7	111.65	88.5	0.793	0.147	0.82	0.093	13.01	2.34

Table (4-71): Reservoir Cuttoff results for well 7

Pay summary										
Zone Name	**Top**	**Bottom**	**Gross**	**Net**	**N/G**	**Av phi**	**Av sw**	**Av Vcl Ari**	**Phi*H**	**PhiSo**
SO-1	2031.9	2039.3	7.4	0	0	-	-	-	-	-
SO-2	2045.8	2051.46	5.66	0.61	0.108	0.16	0.376	0.13	0.1	0.06
SO-3	2151.3	2164.54	13.24	0	0	-	-	-	-	-
SO-4	2166.98	2172.2	5.22	0	0	-	-	-	-	-
SO-5	2174	2177.95	3.95	1.07	0.27	0.156	0.393	0.026	0.17	0.1
SO-7	2218.2	2239.1	20.9	0.15	0.007	0.13	0.5	0.183	0.02	0.01
SO-8	2248.81	2270	21.19	0	0	-	-	-	-	-
SO-9	2276.9	2282.5	5.6	0	0	-	-	-	-	-
SO-10	2285.4	2300.94	15.54	0.91	0.059	0.158	0.439	0.011	0.14	0.08
SO-11	2461.11	2467.7	6.59	0	0	-	-	-	-	-
All zones	2031.9	2467.7	111.65	2.74	0.025	0.156	0.409	0.053	0.43	0.25

Table (4-72): Pay Cuttoff results for well 7

Observations:

well 17 has complicated and heterogeneous data since the SCAL results shows good identification of hydrocarbon while the cutoff results shows high water saturation (80%) on account of the shale content effects the porosity calculations and drop the readings of resistivity causing high water saturation ;hence the SCAL results are more reliable and accurate.

Fig (4-93): Cuttoff for well 7 SO-1 and SO-2

Fig (4-94): Cuttoff for well 7 SO-3, SO-4, SO-5 and SO-6

Fig (4-95): Cuttoff for well 7 SO-7, SO-8, SO-9 and SO-10

4.7 Summary of the Results:

Analysis / Test	Enquiries	Result		
		well 3	well 7	well 1
Relative Permeability	Initial water saturation (S_{wi})		0.352	0.385
	Critical oil saturation (S_{or})		0.263	0.227
	Oil permeability at initial water saturation (K_{ro} @S_{wi})		1	1
	Water permeability at critical oil saturation (K_{rw} @S_{or})		0.156	0.082
	Wetting phase		Water wet	Water w
Capillary Pressure	Number of phases		Two phase	Two pha
	Transition zone height (m)		140	190
Well Logging	Number of target zones	four zones	eleven zones	Four zones
	The best zone of target zones	zone 3 (SA-3)	zone 2 (SO-2)	zone 2 (S-2)
	Average porosity of the best zone (ϕ)	0.217	0.16	0.241

	Average saturation of the best zone (S_w)	0.26	0.376	0.213
	Average shale volume of the best zone (V_{sh})	0.242	0.13	0.165

Table (4-73): Summary of the Results

5.1 Conclusion:

Formation evaluation is process of recognizing a commercial well when we drill one. In this research I evaluate Bentiu Formation from Muglad Basin in Sudan from well log data and core analysis data for three wells.

From relative permeability and capillary pressure analysis that were conducted on the fifteen core plugs that were taken from Bentiu Formation, along with well logging data, we were able to conclude the following points:

- Oil displacement efficiency is anticipated to be economical since formation is water – wet.
- Two phases (oil + water) will be present at the start of production and no single phase (oil) is expected to be solely produced.

- Initial water saturation for south Annajma 7 is 0.3521 while the residual oil saturation is 0.2625 and for south Annajma 17 S_{wi} is 0.385 and S_{or} is 0.227 which reprehensive fine amount and additional methods such as enhanced oil recovery may need later.

From well logging analysis

(South Annajma 3, south Annajma 7, and south Annajma 17) are good reservoir formations because they have good porosity and hydrocarbon saturation but it has fine shale volume.

It is obviously that the data are complicated and leak especially south Annajma 7 which indicates high water saturation at the well logging results because of the high shale content which drop the reading of resistivity lead to high water saturation while the core analysis shows the exact opposite.

5.2 Recommendations:

One of the common, and most important, goals that all reservoir studies aim is to minimize the amount of uncertainity associated with these studies to a tolerable level. It is, therefore, one of our top recommendations to advise and suggest some methods to fulfill that requirement:

- First, it is recommended for future studies to increase the number of core plugs to more accurately describe the reservoir.
- All calculations and graphical representation of the results on this research were performed using Microsoft™ Excel. We recommend considering this software package as the first choice for performing similar tasks.
- Also recommended to increase the number of wells since the minimum wells need to make a model by interactive petrophysics is six wells.

References:

1. Tarek Ahmed , (2006) Reservoir Engineering Handbook .third edition.USA: gulf professional publishing.
2. Torsaeter ,O. & Abtahi, M. (2003) Experimental Reservoir Engineering Laboratory Work Book . Norweg: Norwegian University of Science and Technology.
3. MOSAB, H. A.M. et al. (2011) Conventional and Special Core Analysis Project . Sudan: Sudan University of Science and Technology .
4. Ronalad, N. (1990)Modern Well Test Analysis . fourth edition . California: Palo Alto.
5. Stewart, G. s. t., (1981) The Application of Repeat Formation Tester to the Analysis of Natural Fractured Reservoir, Conference Paper, San Anton: society of petroleum engineers.

6. Mauro Gonfalini. (2005) the fundamental role of formation evaluation in the E&P process, lecture to styped, Italian section: society of petroleum engineers.
7. Browne, S.E. and Fairhead, J.D, (1983) Gravity study of the Central African Rift System: a model of continental dis-ruption.The Ngaoundere and Abu Gabra Rifts.
8. China National Logging Corporation (CNLC),(2006) Principle of wireline logging technology, No.101, Anli Road Chaoyang District,Beijing 100101, P.R.China.
9. Dou Lirong,(2005) Formation mechanism and model of oil and gas accumulations in the Melut Basin, Sudan. Bulletin of Mineralogy, Petrology and Geochemistry.
10. EISAWI, A.A, (2007) Alynological and palaeoenvironmental interpretation of the Late Cretaceous to Tertiary strata of the Melut Basin (southeast Sudan), Unpublished PhD thesis. Technische Universität. Berlin.
11. Fairhead,J.D, (1988) Mesozoic plate tectonic reconstructions of the central South Atlantic Ocean: The role of the West and Central African rift system.
12. Haworth, E., (1913) Special report on well waters in Kansas: Kansas Geological Survey Bulletin. James J. Funk and Servet Unalmiser, 1998, SPE Reservoir Evaluation & Engineering Volume 9.
13. Klitzsch, E. and P. Wycisk, 1987. Geology of the sedimentary basins of northern Sudan and bordering areas. Berliner Geowissenschaftliche Abhandlungen, Reihe A, v.
14. McHargue, T., Heidrick, T. and Livingston, J., (1992) Tectonostratigraphic development of the Interior Sudan rifts, Central Africa. In: P.A Ziegler (Editor), Geodynam-ics of Rifting, Volume II. Case History Studies on Rifts: North and South America and Africa.

15. APPENDIX

16. 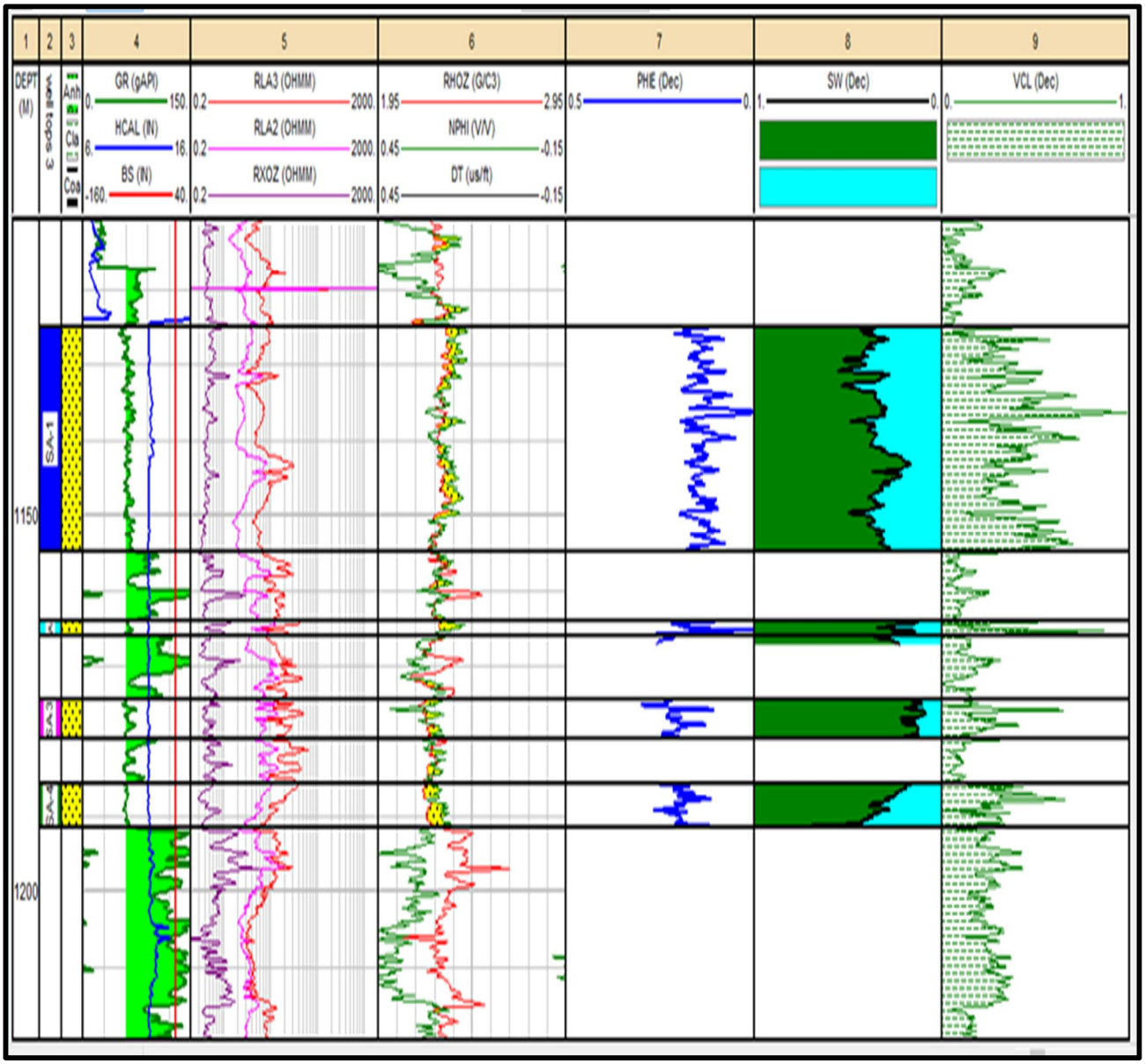

17. Figure (1): Shows log presentation for well 3

18.

19.

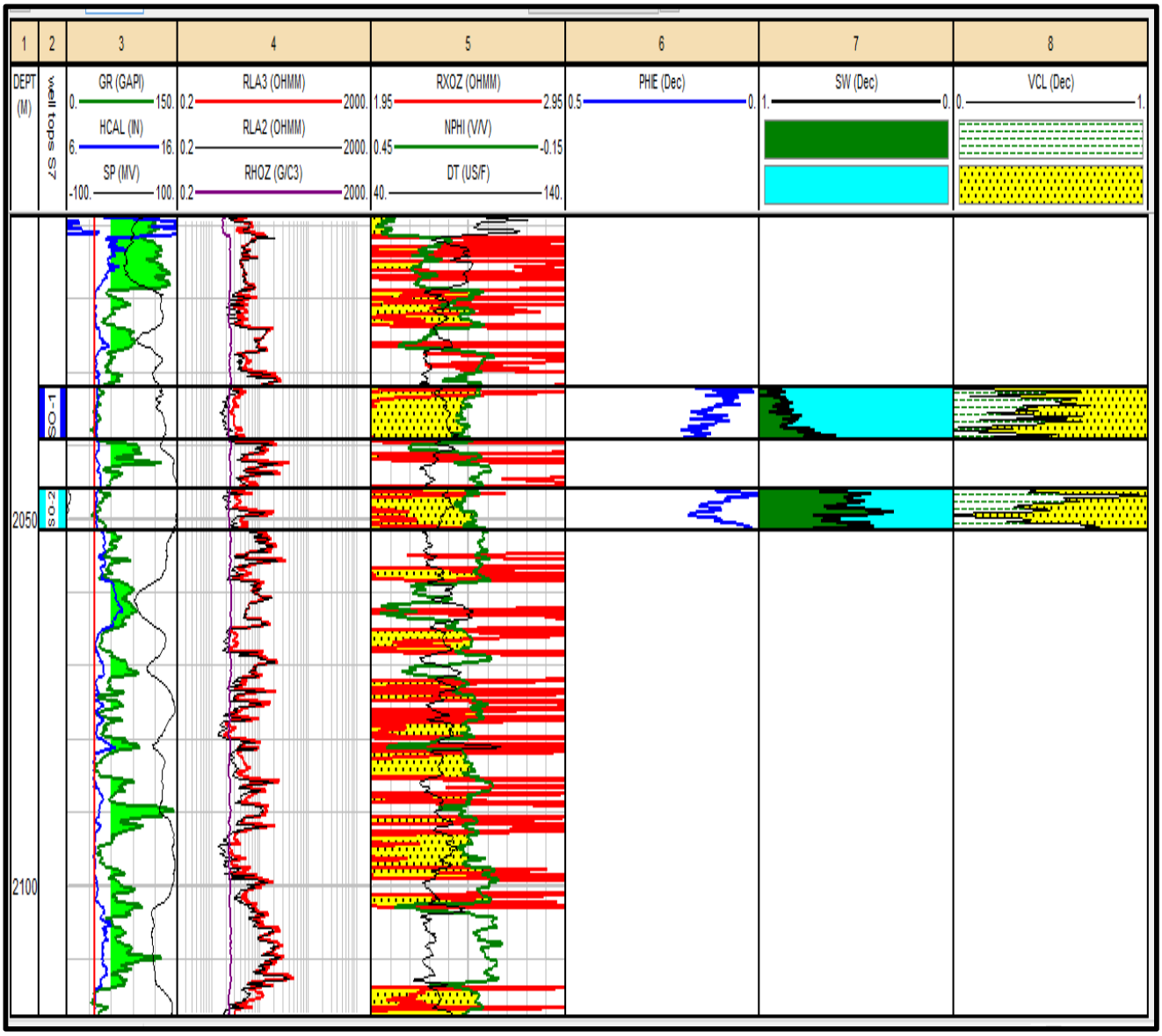

20.

21. Figure (2): Shows log presentation for well 7 zones 1and 2

22.

23. 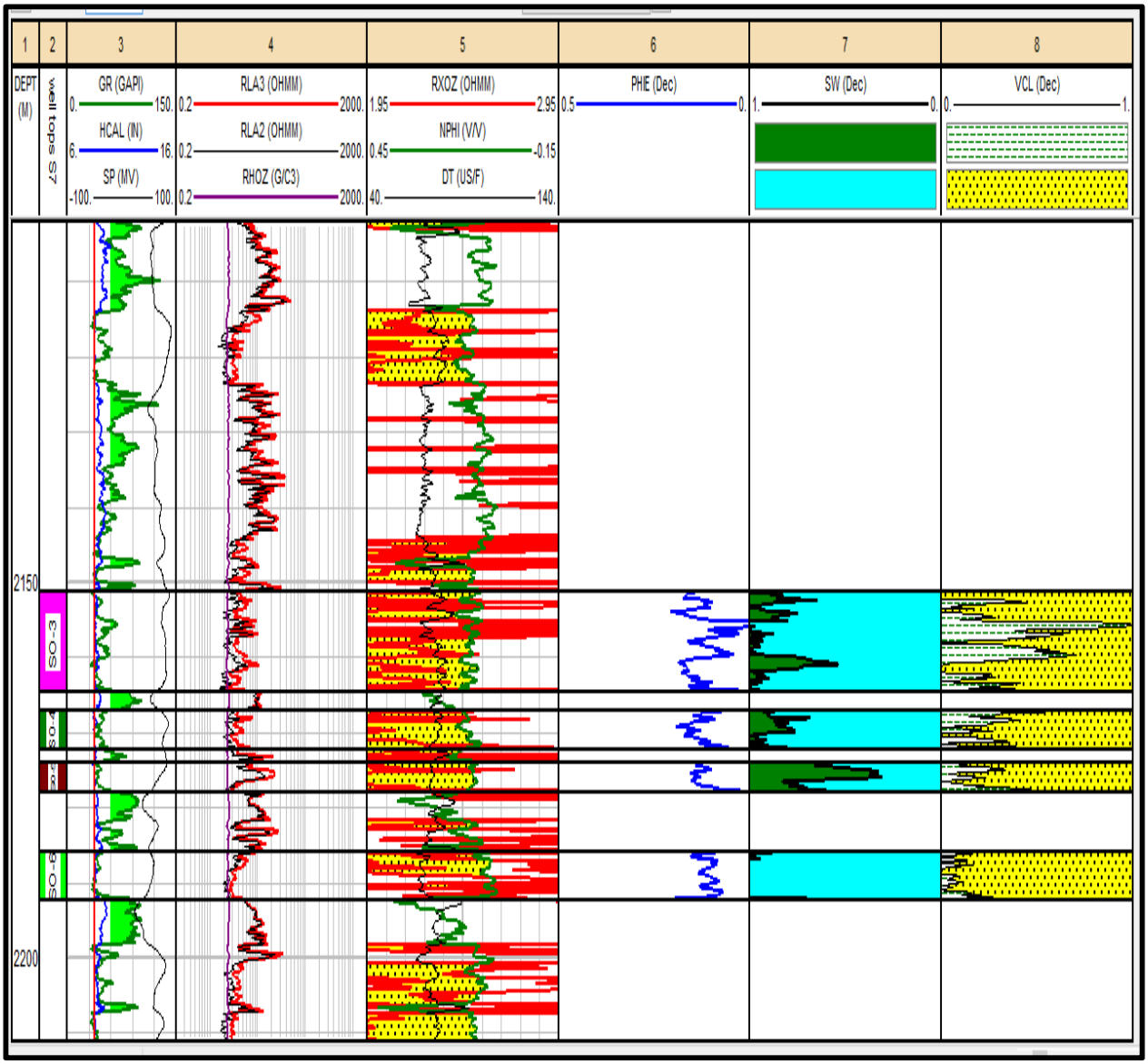

24. Figure (3): Shows log presentation for well 7 zones (3, 4,5and 6)

25.

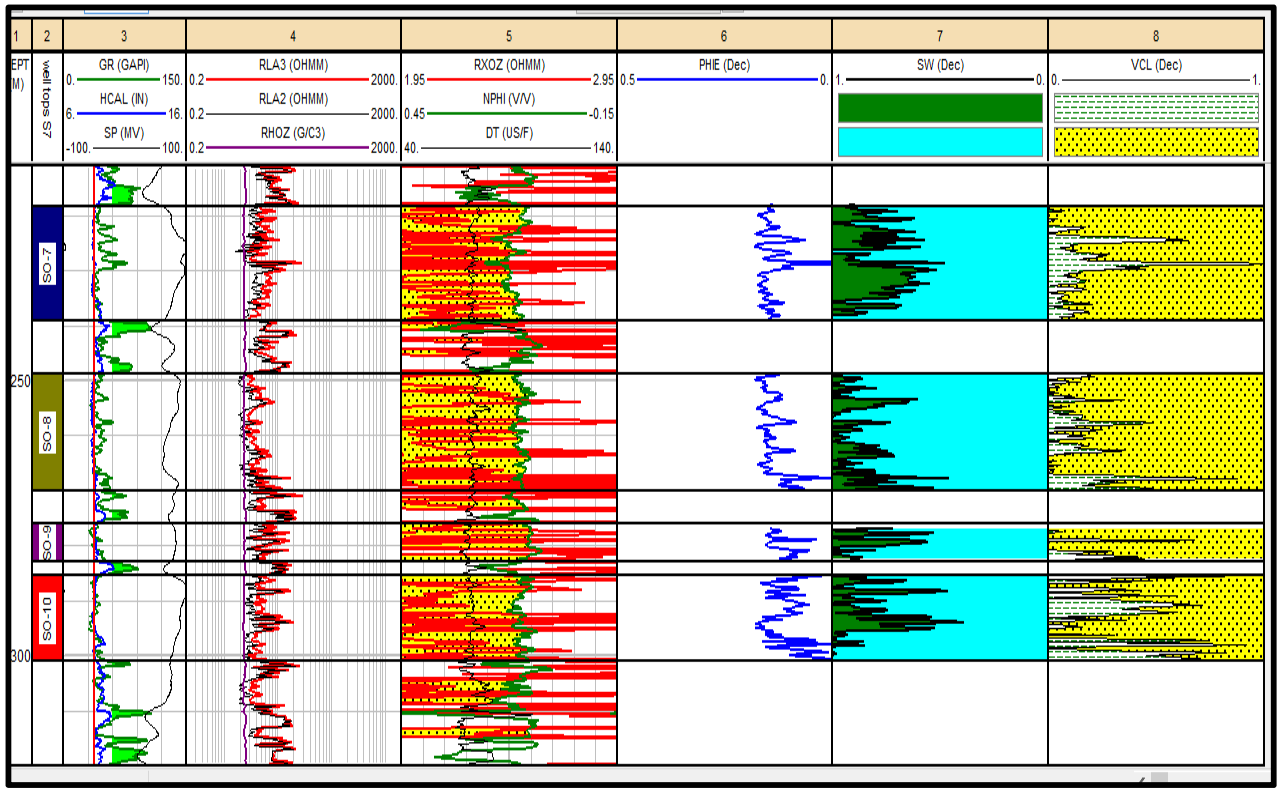

26.

27. Figure (4): Shows log presentation for well 7 zones (7, 8,9and 10)

28.

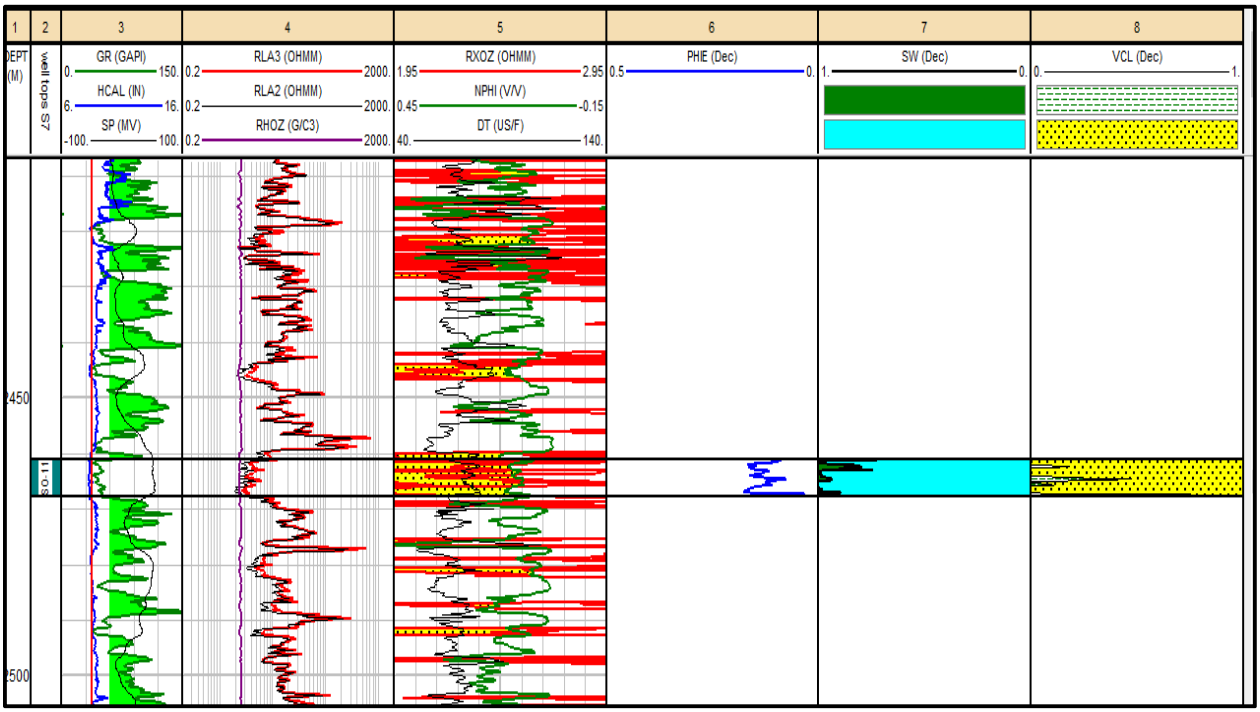

29.

30. Figure (5): Shows log presentation for well 7 zone 11

31. 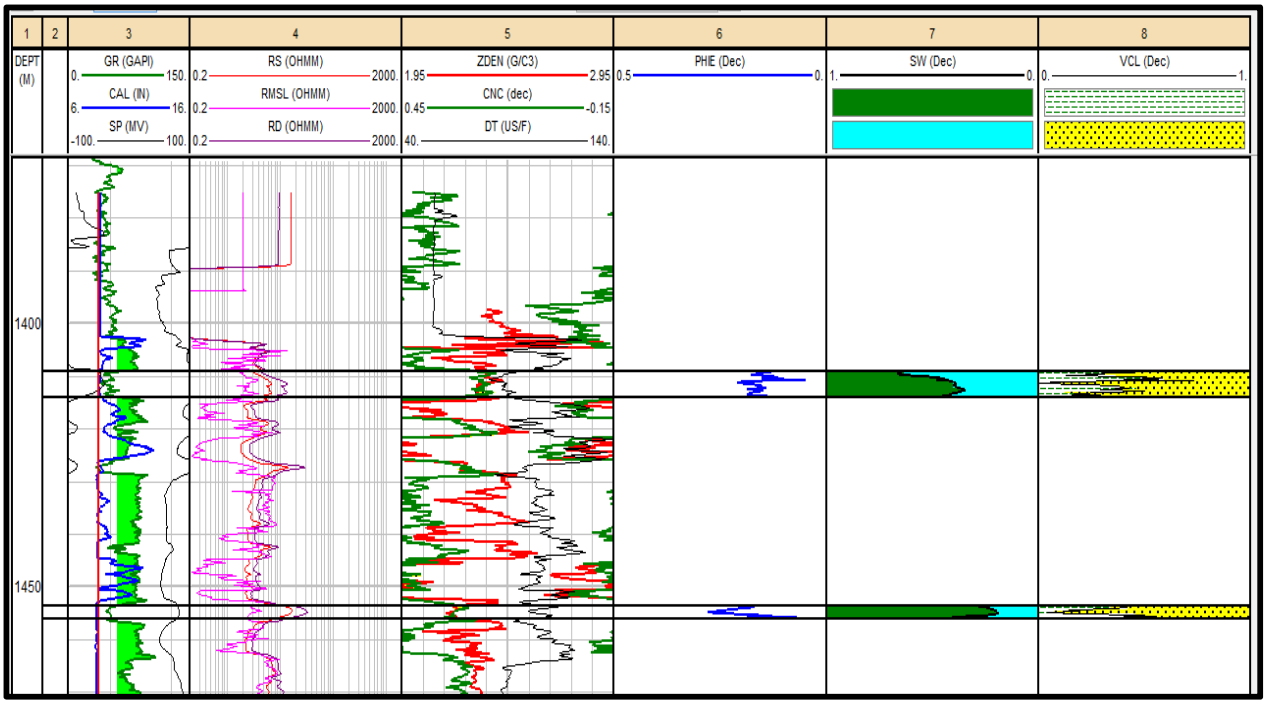

32. Figure (6): Shows log presentation for well 7 zones 1and 2

33.

34. 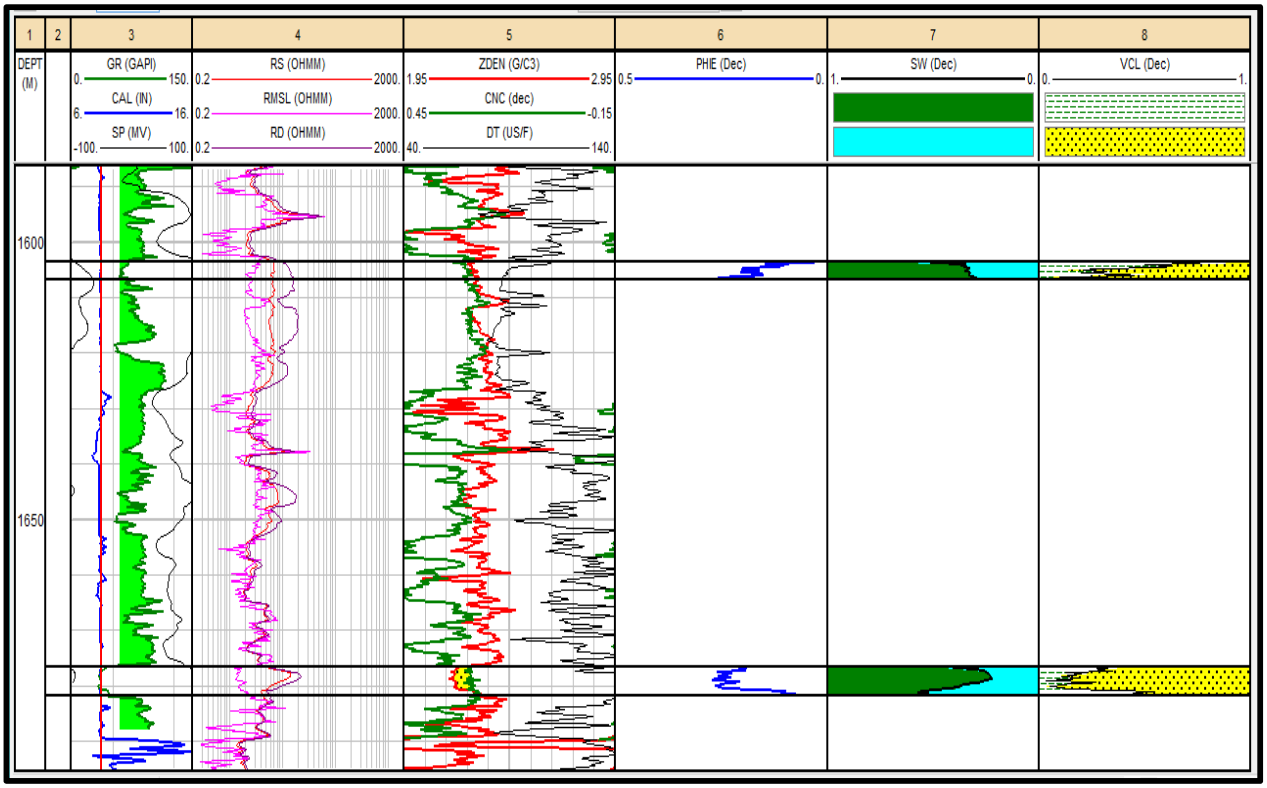

35. Figure (7): Shows log presentation for well 7 zones 3 and 4

36.